Current Research in Toxicology 4 (2023) 100101

Contents lists available at ScienceDirect

Current Research in Toxicology

journal homepage: www.journals.elsevier.com/current-research-in-toxicology

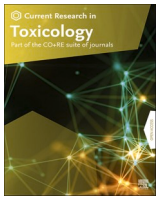

Lung surfactant as a biophysical assay for inhalation toxicology

James Y. Liu, Christie M. Sayes *

Department of Environmental Science, Baylor University, Waco, TX, USA

A B S T R A C T

Lung surfactant (LS) is a mixture of lipids and proteins that forms a thin film at the gas-exchange surfaces of the alveoli. The components and ultrastructure of LS contribute to its biophysical and biochemical functions in the respiratory system, most notably the lowering of surface tension to facilitate breathing mechanics. LS inhibition can be caused by metabolic deficiencies or the intrusion of endogenous or exogenous substances. While LS has been sourced from animals or synthesized for clinical therapeutics, the biofluid mixture has also gained recent interest as a biophysical model for inhalation toxicity. Various methods can be used to evaluate LS function quantitatively or qualitatively after exposure to potential toxicants. A narrative review of the recent literature was conducted. Studies focused whether LS was inhibited by various environmental contaminants, nanoparticles, or manufactured products. A review is also conducted on synthetic lung surfactants (SLS), which have emerged as a promising alternative to conventional animal-sourced LS. The intrinsic advantages and recent advances of SLS make a strong case for more widespread usage in LS-based toxicological assays.

Introduction to lung surfactant

Discovery of lung surfactant

Lung surfactant (LS) is a mixture that coats the surface of the distal regions of the lung where gas exchange occurs. It was first reported on in 1929 by von Neergaard, who noted that surface tension was a critical property of the lung's ability to expand and contract. (Neergaard, 1929) However, it was not until much later that the importance of LS became more recognized, starting with a report by Pattle in 1955 and early connections between surfactant dysfunction and adverse conditions such as atelectasis (partial or total collapse of the lung) and respiratory distress syndrome (RDS). (Pattle, 1955; Avery and Mead, 1959) Various studies followed that elucidated the composition of LS and investigated its biophysical properties. (Scarpelli, 1995). Table 7.1.

Composition and properties

LS lines the surface of alveoli in the lungs (Fig. 3.1) and is typically found to consist of approximately 79 % phospholipids, 13 % neutral lipids, and 8 % proteins. (Parra and Perez-Gil, 2015).

Lipids

Phospholipids. Zwitterionic dipalmitoyl phosphatidylcholine (DPPC) and other phosphatidylcholines (PC) account for the majority of LS by mass. Anionic phosphatidylglycerols (PG) are another significant phospholipid component. Films of DPPC pack in a more ordered fashion in response to compression compared to other phospholipids, indicating an important role achieving low surface tension. The other phospholipid components are thought to contribute fluidity, surface adsorption, and other important properties of LS. (Goerke, 1998; Veldhuizen et al., 1998).

The composition of LS varies across different species. In addition to phosphatidylcholine and phosphatidylglycerol, LS may contain phosphatidylinositol, phosphatidylserine, phosphatidylethanolamine, and phospholipid derivatives such as lysophosphatidylcholine and lysophosphatidic acid. The phosphatidylcholine content is reported to be fairly well conserved across human, bovine, ovine, leporine, and murine samples, while the content of other components fluctuates widely. (Veldhuizen et al., 1998).

Neutral lipids. Neutral lipids, predominantly cholesterol, are the next largest component of LS by mass. Experimental evidence indicates that neutral lipids also contribute to fluidity and adsorption, but not lowered surface tension. There has generally been less research interest on the function of neutral lipids in LS compared to phospholipids or proteins. (Goerke, 1998; Veldhuizen et al., 1998).

Proteins

Surfactant protein A. Surfactant protein A (SP-A) is a collectin (collagen-

* Corresponding author at: Baylor University, Department of Environmental Science, One Bear Place # 97266, Waco, TX 76798-7266.
E-mail address: Christie_sayes@baylor.edu (C.M. Sayes).

https://doi.org/10.1016/j.crtox.2022.100101
Received 25 September 2022; Received in revised form 21 November 2022; Accepted 20 December 2022
Available online 23 December 2022

containing C-type lectin) encoded by two genes with 96 % identical amino acid sequences. SP-A forms trimers which further arrange into an octadecamer "bouquet" structure. SP-A is important to the formation of tubular myelin, an ordered surfactant structure in the alveolar space, and the regulation of surfactant homeostasis. SP-A is suspected to defend against lung injury by preventing surfactant inactivation and assisting innate immune response to pathogens. (Khubchandani and Snyder, 2001; Mason et al., 1998; Kingma and Whitsett, 2006).

Surfactant protein B. Surfactant protein B (SP-B) is a 79-residue member of the amphipathic saposin-like protein family. Its genetic sequence is first transcribed as a 42 kDa precursor before being cleaved into an 18 kDa mature form. Its tertiary structure has a "saposin fold" consisting of 4–5 α-helices linked by disulfide bonds. While the complete 3D structure is not known, a combination of NMR, X-ray crystallography, and homology modelling have indicated that SP-B likely folds into a "closed" conformation with two "leaves" of α-helices. This structure is hypothesized to promote surfactant activity. SP-B forms homodimers and is known to play roles in surfactant spreading, phospholipid recycling, membrane permeability, respiratory cell gene expression, and the structure of tubular myelin. (Hawgood et al., 1998; Walther et al., 2016; Whitsett et al., 1995; Martinez-Calle et al., 2021; Young et al., 1992).

Surfactant protein C. Surfactant protein C (SP-C) is a highly hydrophobic 35-residue protein expressed exclusively by type II alveolar cells. SP-C is first transcribed as a 21 kDa precursor before being cleaved to a 4 kDa secretory protein with an α-helical domain. SP-C is regulated by inflammation and shares many similar surface tension lowering properties as SP-B. Whereas SP-B is primarily found to act at the surface of membranes, SP-C exhibits transmembrane action. SP-C disrupts lipid packing, promoting lipid migration between membrane sheets. SP-C deficiency is associated with RDS and other diseases. (Mulugeta and Beers, 2006; Johansson, 1998; Beers and Fisher, 1992).

Surfactant protein D. Surfactant protein D (SP-D) is an immune system collectin, much like SP-A. SP-D has a native cross-shaped arrangement of four homotrimeric units with long triple-helical arms. SP-D binds to carbohydrates and lipids, playing respective roles in lung defense by binding to viral, bacterial, and fungal glycoconjugates as well as lipid recycling. SP-D is also indicated in the modulation of allergic responses. The differences in properties and function of SP-D compared to the other surfactant proteins may warrant conceptualization as distinct from the surfactant system. SP-D lipid binding is more restricted, and it can be easily separated from LS. SP-D is found in the endoplasmic reticulum of type II cells and in the secretory granules of nonciliated bronchiolar cells but not in LS lamellar bodies or tubular myelin. (Mason et al., 1998; Crouch, 1998; Crouch, 2000; Hartl and Griese, 2006).

Surfactant microstructure

Microstructures in LS primarily consist of lamellar bodies, tubular myelin, and small vesicles. Lamellar bodies range from 1 to 2 μm in size and store phospholipids (primarily PC and PG) as tightly packed, concentric sheets. Tubular myelin structures are lipid-rich, about 2 to 3 μm in size, and consist of ordered lattices of square tubules. (Young et al., 1992; Castillo-Sanchez et al., 2021; Weaver et al., 2002; Poulain et al., 1992).

Function, dysfunction, and applications of lung surfactant

Biophysical function of surfactant

The alveolus of the mammalian lungs is a fragile structure, with a high surface area to facilitate gas exchange. At the air-liquid interface, surface water molecules experience a high cohesive force due to a large difference between interactions with the bulk liquid phase and the vapor phase. This is the basis for surface tension, which must be overcome to create new exposed surface area when the alveolus expands. The main function of LS is to reduce this surface tension, allowing respiratory mechanics to occur without collapse of the alveoli. At the end of expiration, pressure is typically assumed to reach a maximum while surface tension is near zero. Amphiphilic molecules such as phospholipids form a thin film and displace surface water molecules, reducing surface tension. The various surfactant proteins organize and stabilize the LS structure, facilitate recycling, and promote rapid adsorption. (Parra and Perez-Gil, 2015; Goerke, 1998; Autilio and Perez-Gil, 2019).

Fluctuating surface tension gradients in LS induce asymmetric Marangoni flows. These oscillating motions in thin liquid layers can result in convective mass transfer, pushing inhaled particles out of the alveolus. Displacing deposited particles up into ciliated airways is an important mechanism for clearance. This displacement is affected by particle size and surface chemistry. (Gradoń and Podgórski, 1989; Sosnowski, 2018).

Biochemical function of surfactant

When nanoparticles enter the bloodstream, plasma proteins bind to the surface to form a structure known as the protein corona. The protein corona plays a critical role in the recognition and clearance of the particles by the immune system. When particles are inhaled, components of the lung surfactant also form a corona, though the composition differs from that formed by plasma. (Rampado et al., 2020; Kapralov et al., 2012).

Proteomic analysis of LS coronas bound to nanoparticles (separated

Table 7.1
Synthetic lung surfactant formulations. Each ingredient is categorized into a general class and listed by both abbreviated and full name. Columns under "Synthetic Lung Surfactant Formulation" represent different individual commercial or experimental formulations. Acronyms include artificial lung expanding compound (ALEC); Chiesi Farmaceutici 5633 (CHF5633), Forbes group of King's College London (F-KCL).

Class	Ingredient	Formula	Full Name	Synthetic Lung Surfactant Formulation						
				ALEC	Exosurf	Surfaxin	Venticute	CHF5633	Minisurf	F-KCL
Lipid	DPPC	$C_{40}H_{80}NO_8P$	dipalmitoyl phosphatidylcholine	✓	✓	✓	✓	✓	✓	✓
	DPPG	$C_{38}H_{74}NaO_{10}P$	dipalmitoyl phosphatidylglycerol							✓
	POPC	$C_{42}H_{82}NO_8P$	palmitoyloleoyl phosphatidylcholine						✓	
	POPG	$C_{40}H_{77}O_{10}P$	palmitoyloleoyl phosphatidylglycerol	✓		✓	✓	✓	✓	
	Cho.	$C_{27}H_{46}O$	cholesterol							✓
Fatty Acid	Pal. Aci.	$C_{16}H_{32}O_2$	palmitic acid			✓	✓			
Fatty Alcohol	Cet. Alc.	$C_{16}H_{34}O$	1-hexadecanol		✓					
Polymer	Tyl.	$C_{17}H_{28}O_3$	tyloxapol		✓					
Protein	IgG		immunoglobulin G							✓
	Alb.		albumin							✓
	Tra.		transferrin							✓
	aSP-B		surfactant protein B analog					✓		
	aSP-C		surfactant protein C analog					✓		
	rSP-C		recombinant surfactant protein C				✓			

magnetically) detected and quantified numerous proteins. The five most abundant were SP-A, serum albumin, sodium-dependent phosphate transport protein 2B, tubulin alpha-4A chain, and fibronectin. Comparing protein coronas formed by LS and crude plasma, only 4 of the top 20 abundant proteins are shared. LS corona also contains a major lipid component, the most abundant of which are phosphatidylcholine and phosphatidylinositol. The protein:lipid ratio of the LS corona is estimated to be 1:10. From a molecular function standpoint, LS corona has enhanced catalytic and structural activity, plasma corona has enhanced antioxidant and enzyme regulation activity, and both have a strong emphasis on binding. (Raesch et al., 2015).

Coarse-grained molecular dynamics simulations found that the structure of LS corona varied with particle surface chemistry. Lipids arranged in a monolayer conformation on hydrophobic polystyrene nanoparticles but arranged in a bilayer on hydrophilic silver nanoparticles. Surfactant proteins B and C are found to interact with the corona lipid layers in parallel and transmembrane orientations respectively, in agreement with their behavior in bulk LS. SP-A is found to bind to nanoparticle surfaces via the carbohydrate recognition domain exclusively. Once the corona is formed, the subsequent pharmacokinetics of inhaled nanoparticles are altered. The LS corona increases the size of nanoparticles, reduces hydrophobicity, and increases the density of surface phosphate groups. These changes mitigate inflammatory potential and promote recognition and clearance of inhaled nanoparticles. (Hu et al., 2017).

In addition to biotransformation, LS plays a role in innate immune function. Lung collectins SP-A and SP-D have been shown to bind directly to the surface oligosaccharides, glycoproteins, or lipid moieties of various microorganisms including gram-negative bacteria, gram-positive bacteria, fungi, and viruses. SP-A and SP-D stimulate the phagocytosis of bacteria, viruses, and damaged lung cells by alveolar macrophages. They also have been shown to independently inhibit the growth of bacteria and fungi by increasing microbial membrane permeability. SP-A and SP-D have also been shown to modulate both pro-inflammatory and anti-inflammatory responses to pathogens. (Wright, 1997; Eggleton and Reid, 1999; Takahashi et al., 2006).

Surfactant inhibition

LS function may be diminished when it interacts with endogenous substances such as serum proteins (leaked into the alveolar space during respiratory distress syndrome) or exogenous substances such as nanoparticles or other inhaled pollutants. This decrease in LS function is known in the literature as “inhibition” or “inactivation”. Inhibited LS may fail to reach low surface tension under compression or fail to respread during expansion. Under this paradigm, surfactant inhibition is typically recognized as an elevated minimum surface tension after LS is exposed to agents of concern and compression cycles. The underlying mechanisms behind inhibition are not fully understood but progress is ongoing using microscopy, spectroscopy, proteomics, and other classes of techniques. (Zuo et al., 2008; Ravera et al., 2021).

Serum proteins

In RDS and related pathologies, the alveolar-capillary barrier may become compromised, allowing proteins from blood serum to leak into the internal space and interact with LS. Extensive study has shown the inhibition of surfactant by albumin, fibrinogen, and hemoglobin. These proteins compete with phospholipids for surface presence, disrupting monolayers and therefore inhibiting the LS. (Holm et al., 1988; Warriner et al., 2002).

Lipids

Various lipids such as unsaturated phospholipids, lysophospholipids, bile acids, and cholesterol have been implicated as LS inhibitors. These lipids are found to disrupt LS function by fluidizing phospholipid monolayers or generating DPPC-rich condensed domains, decreasing film stability. These lipids may be introduced by cell secretions during RDS or as a component of meconium aspirated by neonates during delivery. (Clark et al., 1987; Hite et al., 2005; Malcharek et al., 2005).

Meconium

Meconium is early stool defecated by infants that may be passed into the amniotic fluid. Aspiration of meconium during delivery is a widely implicated cause of neonatal RDS. Meconium has a complex and variable composition and is known to inhibit LS. (Rubin et al., 1996; Sun et al., 1993).

Air pollutants

Air in both outdoor and indoor environments contains a variety of gases, particles, and biological pathogens that can cause adverse health effects when inhaled. Nanoparticles that deposit in the lungs may alter Marangoni flows or cause oxidative stress and the subsequent generation of reactive oxygen species (ROS). LS phospholipids and proteins have shown decreased function after oxidation. Hydrophobic particles may also disrupt tight packing by becoming trapped in the hydrophobic phases of LS. Adsorption of LS components to particle surfaces is thought to play a role in clearance from the lungs, but particle morphology or surface properties may hinder proper clearance. (Parra and Perez-Gil,

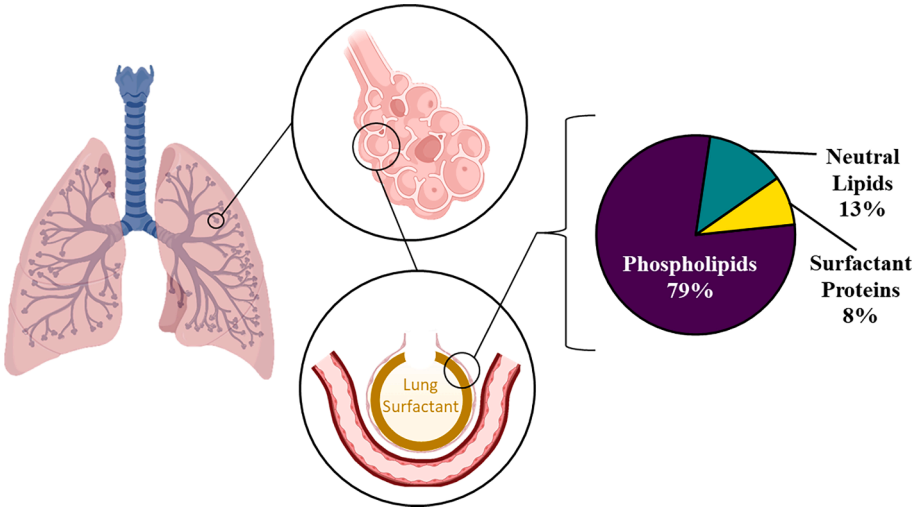

Fig. 3.1. Location and composition of lung surfactant. Left: illustration of the human lungs and trachea; upper middle: illustration of alveolar cluster; lower middle: illustration of individual alveolus with lung surfactant lining the surface; right: circle chart with composition of lung surfactant by percentage.

2015; Guzmán, 2022).

Pathogens

Substances produced by pathogens (*e.g.* bacteria, fungi) may also interfere with LS. For example, bacterial membrane lipopolysaccharide (LPS) may biophysically inhibit LS by decreasing lipid layer stability. (Canadas et al., 2011).

Surfactant metabolism

After approximately 24–34 weeks of gestation, type II alveolar epithelial cells undergo differentiation regulated by transforming growth factor beta (TGF-β) signaling and glucocorticoid levels. During gestation, a fully functioning pulmonary system is not needed as oxygen is supplied by the umbilical cord. The first breath after birth stimulates the release of lamellar bodies into the hypophase layer covering the alveolar epithelium. (Nkadi et al., 2009; King and Chen, 2020).

Dysfunction in surfactant metabolism can result in the underproduction of overproduction of LS components. Underproduction of surfactant can result from premature birth, genetic deficiency, or diseases such as cystic fibrosis. (Chakraborty and Kotecha, 2013; Postle et al., 1999).

The overproduction of surfactant proteins has been observed in the pathogenesis of pulmonary fibrosis, silicosis, and secondary pulmonary alveolar proteinosis after infection by the fungus *Pneumocystis jirovecii*. (Fasske and Morgenroth, 1983; Lesur et al., 1993; Shibasaki et al., 2009).

Surfactant in clinical settings

A variety of commercial formulations for clinical surfactants have been developed and used to treat RDS, acute lung injury (ALI), and related conditions (Fig. 4.1). Preparations are typically categorized as either animal sourced (*ex vivo*) or synthetic in origin.

Neonatal RDS is the most common cause for neonatal intensive care and the leading cause for complications and mortality in preterm infants. Surfactant protein produced by cuboidal type II alveolar epithelial cells is first detected at around 24 weeks of gestation. Preterm infants lack mature surfactant metabolism, leading to a gradient of neonatal RDS incidence dependent on gestational age. RDS occurs in approximately 98 % of babies born at 24 weeks. Surfactant deficiency can also be caused by genetic mutations, typically in genes encoding for SP-B, SP-C, thyroid transcription factor-1 (TTF-1), and ATP-binding cassette subfamily A member 3 (ABCA3). An additional pathway involves genes encoding for granulocyte-macrophage colony stimulation factor (GM-SCF), which is important to the maturation of alveolar macrophages. Surfactant metabolism maturity is also tied to phospholipid turnover and composition. (Chakraborty and Kotecha, 2013; Ainsworth, 2005; Pioselli et al., 2022; Smith et al., 2012; Bernhard, 2016).

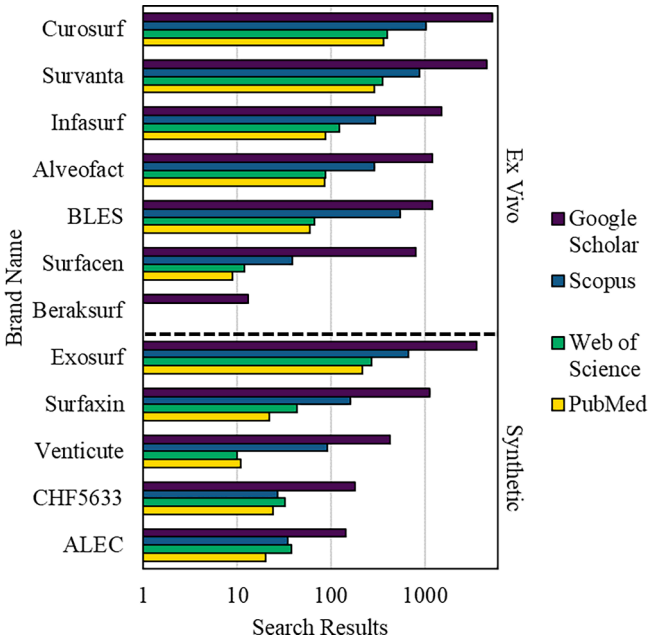

Fig. 4.1. Commercial surfactant brands and their presence in the literature. Brands are divided into two categories, *ex vivo* and synthetic. Results are presented on a log scale from four scientific literature search engines. Acronyms: bovine lipid extract surfactant (BLES); Chiesi Farmaceutici 5633 (CHF5633); artificial lung expanding compound (ALEC).

Early attempts in the 1960s to nebulize DPPC for RDS treatment were unsuccessful. It was not until the 1980s that trials with Surfactant-TA, ALEC, Curosurf, and other preparations showed promising results. As of 2017, only three surfactant preparations were licensed for use in Europe (Survanta, Alveofact, and Curosurf), all derived from animals. The United States licenses four preparations (Survanta, Infasurf, Curosurf, and Surfaxin), of which only one (Surfaxin) is synthetic. Modern surfactant replacement therapies aim to employ delivery methods that are less invasive and more effective. In addition to RDS, trials are expanding to other pathologies such as emphysema and pneumothorax. (Halliday, 2017; Han and Mallampalli, 2015).

Methods to measure lung surfactant function

As the research investigating LS gains momentum, methods to measure LS function have increased in number and improved, contributing to advances in clinical and toxicological contexts. The common concept behind these methods is to simulate an alveolus and empirically determine the surface tension of LS at initial adsorption, minimum, and maximum values. (Ravera et al., 2021).

Langmuir-Blodgett trough

First reported by Langmuir and Blodgett in the early 20th century, the Langmuir-Blodgett trough (LBT) laterally compresses an oil film on the surface of water which is centrally drawn by lifting a submerged vertical plate. Surface pressure can then be measured using a Wilhelmy plate or Langmuir balance configuration. The method has evolved over time with varying materials used for construction and improvements in the measurement apparatus. In the context of LS, design limitations of the LBT restrict it to compression experiments and so it is typically used for phospholipid monolayers rather than complete surfactant experiments. (Langmuir, 2002; Blodgett, 2002; Oliveira et al., 2022).

Pulsating bubble

First reported in 1977 by Enhorning, the pulsating bubble surfactometer (PBS) generates an air bubble at the end of a capillary submerged in a chamber of liquid sample. The bubble is oscillated between fixed radii and surface tension is estimated by the pressure differential across the bubble assuming the Laplace relation for a spherical surface. The PBS provides better simulation of breathing dynamics than the LBT with higher throughput but is limited by inaccuracies at minimum bubble size, film leakage, and fluid opacity. Inhibitory components must also be pre-mixed with the sample, which is not realistic in the context of environmental aerosol exposure. (Enhorning, 1977; Enhorning, 2001).

Captive bubble

First reported by Schurch in 1989, the captive bubble surfactometer (CBS) uses an air bubble inside a glass flow-through cell with a concave hydrophilic ceiling. Internal stirring is used and the bubble is oscillated by hydraulic pressure using a piston from above. The bubble shape is analyzed using the classic Laplace capillary relation. CBS results are

typically presented as isotherms between surface tension and relative area. Due to similar design, the CBS carries many of the same limitations at the PBS. (Schurch et al., 1989; Schürch et al., 1998).

Constrained drop

First reported in 2015 by the Zuo group at the University of Hawaii, the constrained drop Surfactometer (CDS) was developed to study LS inhibition by aerosols. LS is adsorbed to the surface of a pedestal with sufficiently small surface area to minimize the effect of gravity and sufficiently sharp edges to prevent film leakage. Cycling is achieved through a small channel in the center of the pedestal and a motorized syringe setup. The configuration is encased in a clear, sealed chamber heated from the bottom. Droplet shape is monitored by a high-definition camera and aerodynamic particle size is measured by laser diffraction spectroscopy. Whereas the CBS and PBS simulate the alveolus as a bubble of air inside LS, the CDS uses a bubble of LS inside air, allowing closer mimicry of exposure to aerosols. Compression cycles measured by the CDS most resemble those obtained by the CBS. (Valle et al., 2015; Sorli et al., 2016).

Other methods

Fluorescence anisotropy is a technique used to investigate biomolecular motion and kinetics, such as protein-membrane interactions and lipid vesicle fusion or separation. Biomolecules are labeled with fluorescent probes and the change in polarization and resulting decay of fluorescently emitted signal is measured. Fluorescence anisotropy has been applied to the study of LS, including SP-C aggregation and membrane fluidization. (Steiner, 2002; Horowitz et al., 1993; Saenz et al., 2007).

Differential scanning calorimetry (DSC) is a technique used to investigate phase transitions in lipid membranes and other assemblies of biomacromolecules. A sample and reference cell are shielded in an enclosure, each in contact with an individual heater. Temperature sensors and a controller are used to maintain the temperature difference at near zero, with the required heat flow in or out recorded as the calorimetric signal. DSC can be used to probe perturbations in LS membranes. (Spink, 2008; Demetzos, 2008; Canadas et al., 2022).

Viscosimetry is the measurement of viscosity in fluids. Viscometers involve either a stationary sample and mobile object or the inverse, with some method of measuring applied force to calculate dynamic modulus. Viscosimetry has been used to investigate LS lipid layer transitions, the effect of polymer additives to clinical surfactants, and the effect of nanoparticles on LS fluidization. (Alonso et al., 2005; Lu et al., 2009; Thai et al., 2020).

Atomic force microscopy (AFM) scans across a sample using an ultrafine tip mounted on a cantilever. A laser is used to measure the force signal as the tip drags or oscillates across the material surface. For LS, films generated using the LBT technique are transferred to mica sheets for imaging of structural features. (Zhao et al., 2019b; Yang et al., 2018; Wu et al., 2022).

Brewster's angle microscopy (BAM) is used to study the surface layer of liquids. The Brewster's angle of a liquid allows perfect transmission of polarized light. This allows the imaging of structures in the layer near the surface. BAM is typically paired with the LBT technique to study Langmuir films. BAM can capture structural transitions in LS related to biophysical function. (Fang et al., 2020; Hu et al., 2020; Bykov et al., 2022).

Cryogenic transmission electron microscopy (Cryo-TEM) can be used to investigate cross sections of the 3D structure of soft materials. Rapidly frozen samples are sectioned and placed on a grid. An electron beam is focused onto the sample and different operating modes are used to obtain images. Cryo-TEM can capture small structures in LS such as micelles and vesicles. Changes in LS microstructure can infer altered function. (Tchoreloff et al., 1991; Waisman et al., 2007; Braun et al., 2007).

X-ray diffraction (XRD) scatters X-rays through a sample to investigate crystallinity via electron density. For studies on LS, X-ray diffraction has been most used to investigate interactions with serum albumin. (Braun et al., 2007; Larsson et al., 2006; Stenger et al., 2009).

Molecular dynamics use potential functions or force fields to build computer simulations of the physical movements of molecules. Coarse-grained models may be used to reduce computational intensity by grouping atoms or molecules together. Molecular dynamics can study the interactions of particles with LS components (*e.g.,* corona formation) and bilayers (*e.g.* translocation). (Hossain et al., 2019; Yue et al., 2017; Li et al., 2022).

Molecular docking uses shape, flexibility, and affinity to predict the favorability of different orientations for the binding between ligand and target molecules. Molecular docking can indicate binding potential between toxicants and LS proteins. (Li et al., 2021; Rajak et al., 2021).

Narrative review of lung surfactant as a toxicological model

Toxicology aims to determine the potential harmful effects of substances. Toxicity tests are employed to quantify toxic effects in response to exposure conditions (*e.g.,* frequency, duration, route) and dose (amount of substance absorbed) in some model receptor. Advancements in the late 19th and early 20th centuries led to the synthesis of many new chemicals that needed pharmacological testing. This precipitated with the formation of various pharmacology institutions and the systematic breeding of laboratory test animals. New regulations in the mid-20th century further propelled the importance of animal testing in the United States to obtain approval for pharmaceuticals, chemicals, and consumer products. USDA data shows that usage of many animal species peaked in the 1980 s and has declined by over 50 % since. This reflects a major paradigm shift towards rodent models and *in vitro* models. (Khabib et al., 2022; Kinter et al., 2021).

Rodents are the dominant animal model for both toxicological and biomedical research. The Hannover Wistar and Sprague Dawley strains of rat are the most notable competing standards for animal toxicity testing. Due to the cost and labor involved in mammalian models, as well as increasing interest in ecological health (as opposed to human health), a variety of alternative animal models have been explored. Notable examples include zebrafish, roundworms, molluscs, and daphnia. (Khabib et al., 2022; Weber et al., 2011; Ellenbroek and Youn, 2016).

In vitro models for toxicity testing have gained momentum over the past years due to cost, time, complexity, and ethical considerations. Various levels of sophistication are available including monolayers, cocultures, 3D cocultures, and *ex vivo* tissue. The major limitation of *in vitro* systems is poor translation to *in vivo* results. This is due to the absence of immune function, transporters, ligands, extracellular matrix interactions, or other components that affect the behavior of *in vivo* systems. Research using *in vitro* toxicity testing has thus shifted away from monolayers and towards organ explants or organ mimicry. (Jain et al., 2018:; Zucco et al., 1998; Astashkina et al., 2012).

Lung surfactant plays a key role in the development of adverse outcomes following the inhalation of toxic substances. LS-based models introduce physiological aspects that are absent from rudimentary monolayers of pulmonary cells. Hazard identification can be conducted by measuring changes in LS inhibition after direct mixture or aerosol exposure to substances. Preliminary results show that the LS model may be able to predict *in vivo* results for respiratory toxicity. As animal models are now considered a last resort, LS bioassays are a promising toxicological model for inhalation exposure with potential for high-throughput screening. (Guzmán, 2022; Da Silva et al., 2021a; Dwivedi et al., 2014; Sorli et al., 2022).

Review criteria and results

A literature search was performed to identify all relevant studies on the inhibition of lung surfactant by exogenous toxicants. Literature from the past 20 years was sampled by Google Scholar using the query: ["lung surfactant" AND "inhibition" AND "surface tension" AND ("toxicology" OR "toxicity" OR "pollutant")]. A total of 1350 results were returned, of which 303 reviews were discarded. The first 160 results returned were then manually reviewed for relevance, yielding a sample of 50 peer-reviewed research articles. Articles focused on the clinical enhancement of surfactant, therapeutic design, or other non-toxicological studies were excluded. Duplicate results and non-English-language articles were also discarded. All of the following analysis is based on the sample of 50, for which the distribution by publication year is shown in Fig. 6.1.

The techniques utilized across the papers in the sample were analyzed (Fig. 6.2). All papers in the sample employed a quantitative method for studying LS function, with a majority focusing on *in vitro* surface tension (most often using a Langmuir-Blodgett trough or LBT) and a minority focusing on *in silico* methods (namely molecular dynamics and molecular docking). Many *in vitro* studies paired surface tension measurement with a qualitative microscopy technique, with atomic force microscopy (AFM) being the most popular.

Across the sample, a diverse array of toxicants was studied (Fig. 6.3). The two dominant areas of study were environmental contaminants (often complex mixtures) and nanoparticles (often homogenous and well defined). The remainder focused on manufactured products (specific formulations used in industrial, consumer, and medical applications).Fig 7.1-7.3.

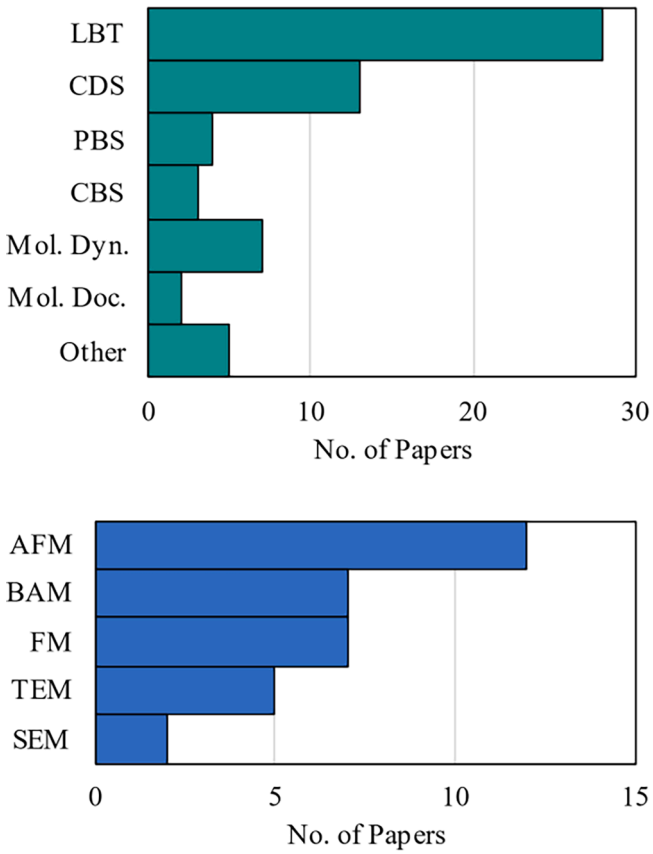

Fig. 6.2. Number of papers utilizing (above) quantitative and (below) qualitative methods to measure surfactant function in response to toxicological exposure across the sample. Quantitative methods consisted of surfactometers, computational modeling, and other techniques. Qualitative methods consisted of microscopy techniques. Acronyms: Langmuir-Blodgett trough (LBT), constrained drop surfactometer (CDS), pulsating bubble surfactometer (PBS), captive bubble surfactometer (CBS), molecular dynamics (Mol. Dyn.), molecular docking (Mol. Doc.), atomic force microscopy (AFM), Brewster's angle microscopy (BAM), fluorescence microscopy (FM), transmission electron microscopy (TEM), scanning electron microscopy (SEM).

Lung surfactant toxicology and environmental contaminants

Combustion products

The combustion of fossil fuels is ubiquitous across human activities, most notably in transportation, electricity generation, and industrial processes. The products of combustion typically include respirable particle aerosols that humans are regularly exposed to in environmental, occupational, and behavioral contexts. Inhalation exposure to combustion products is associated with numerous adverse respiratory health effects and is considered a major global health problem.

The main constituent of combustion residues is carbon. A study with just carbon nanoparticles also observed changes in surface pressure isotherms, compressibility, and phase transitions in LS (Hu et al., 2020).

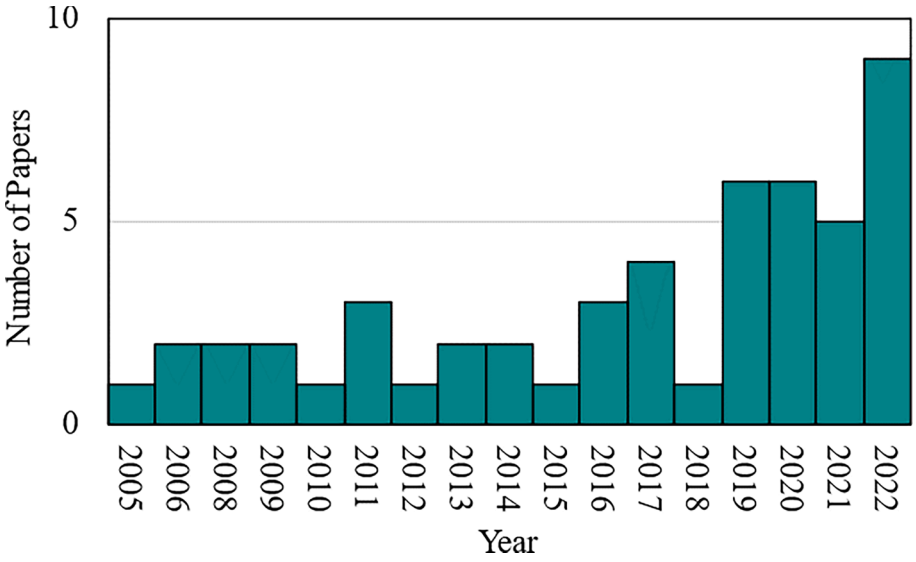

Fig. 6.1. Distribution of the 50 sampled papers by year.

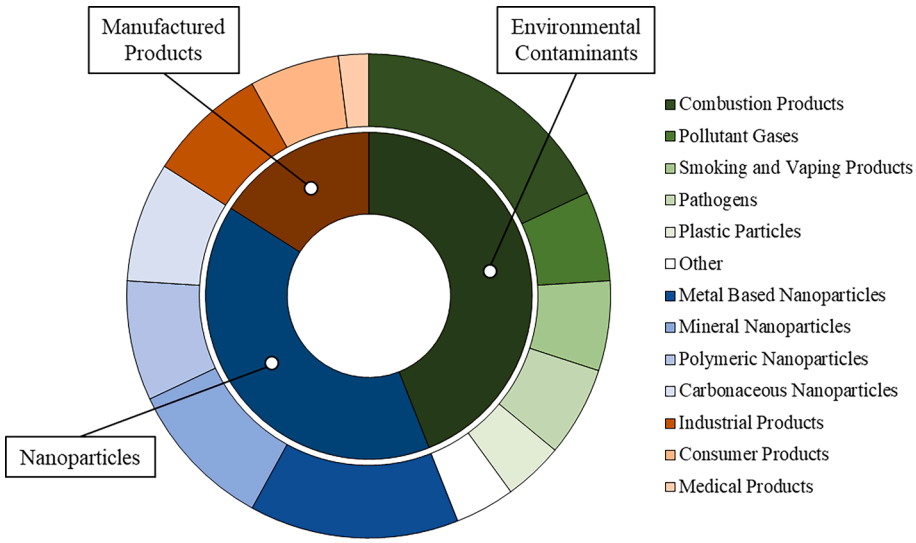

Fig. 6.3. Classifications of toxicants studied in the sample of 50 papers. Results are shown in parallel between major (inner circle, legend overlaid) and minor (outer circle, legend right justified) classifications.

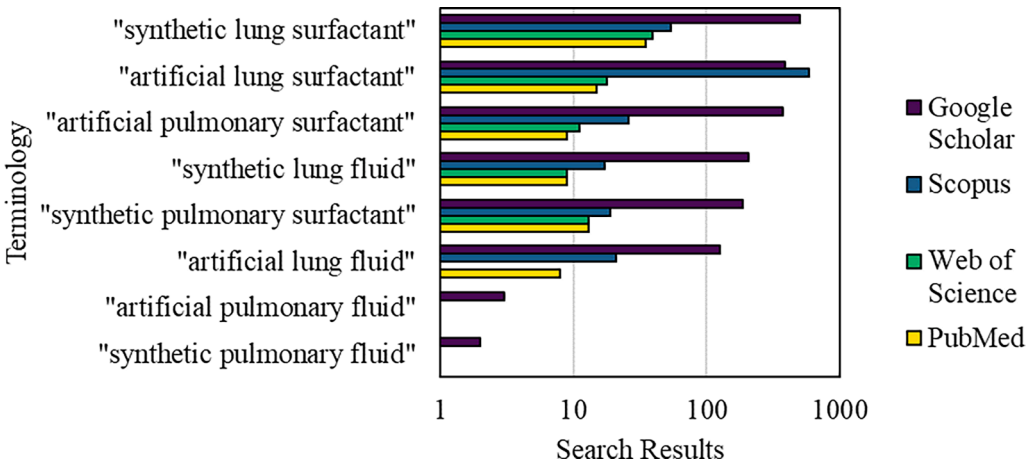

Fig. 7.1. Terminology for surfactants that are not sourced from animals. The vertical axis presents the exact terms that were searched for. Results are presented on a log scale from four scientific literature search engines.

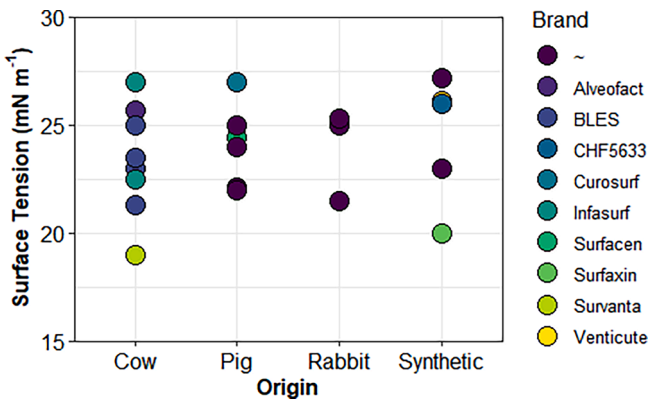

Fig. 7.2. Comparison of literature equilibrium surface tension for surfactant preparations. Values are categorized by animal of origin, with an additional designation for synthetic. (~) denotes non-branded surfactants, such as direct extracts from animal lungs.

Another study looked at three different types of carbonaceous soot particles (Guzmán et al., 2022). Insertion of the particles into LS films in an LBT was observed to modify interfacial cohesion and packing, resulting in inhibited surface tension. Another study exposed LS to a standard diesel particulate matter (DPM) in an LBT (Wu et al., 2022). LS function was assessed by surface pressure isotherms, BAM, AFM, and X-ray photoelectron spectroscopy. Binding with DPPC was studied using calorimetry. The DPM induced expansion at low pressure and condensation at high pressure, with aggregation at the interface between phases and heterogenous fast binding.

Polycyclic aromatic hydrocarbons (PAHs) are often formed during incomplete combustion, and exposure is implicated in serious human health risks such as cancer and cardiovascular disease. An example is the formation of benzo[α]pyrene (BaP) from diesel engines. LS was exposed to DPM and BaP in a PBS, showing significant inhibition of surface activity (Sosnowski et al., 2011). Molecular dynamics simulations were used to elucidate the mechanism, indicating the insertion of BaP into the lipid layer. Another study on BaP corroborated the alteration of surface tension, phase behavior, and interfacial structure in LS (Cao et al., 2021). Solubilization of BaP was found to enhance the consumption of hydroxyl radicals. Anthracene is another PAH and a component of coal tar. LS was exposed to carbon nanoparticles and anthracene (Zhao et al.,

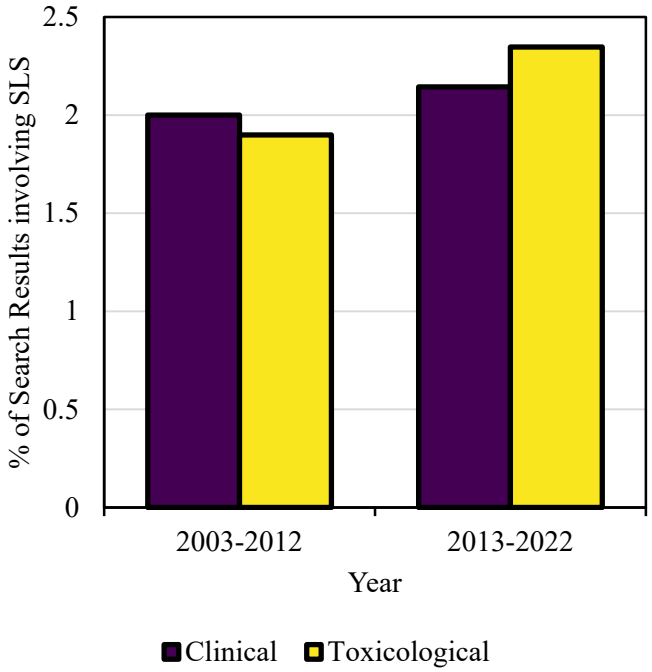

Fig. 7.3. Proportion of LS research mentioning SLS. Results for literature mentioning synthetic lung surfactant are obtained from Google Scholar, filtered by year and inclusion of contextual terms related to clinical or toxicological contexts. These are then divided by the same results for lung surfactant in general.

2019a). LBT and BAM techniques showed that surface tension, phase behavior, and foaming ability of the LS were altered. The solubilization of anthracene was found to play a key role in the inhibitory effects.

A variety of combustion processes can generate carbonaceous particles that contain metals or other contaminants. Soot particles from industrial smelting are often heavy metal rich. LS was exposed to these soot particles in an LBT, finding that heavy metal solubilization by bovine serum albumin exacerbated LS inhibition (Fang et al., 2020). Residual oil fly ash (ROFA) is emitted by the burning of low-grade oil, containing metal salts as well as nitrogenous compounds. Viscosimetry of LS via an interfacial stress rheometer showed decreased elasticity and viscosity (indicative of gelation) after exposure to ROFA (Anseth et al., 2005). Biofuel combustion is commonly used for household cooking in rural India. LS in an LBT was exposed to the dried particulates from this combustion, resulting in increased minimum surface tension (Kanishtha et al., 2006).

Pollutant gases

Ozone is a ubiquitous pollutant gas known to increase respiratory disease and mortality. Using an LBT and neutron reflectivity, ozone was observed to damage unsaturated phospholipid tails, causing them to reverse orientation and increase LS surface pressure at the air-liquid interface (Thompson et al., 2013).

Volatile organic compounds (VOCs) are widely encountered environmental pollutants that are tied to a variety of adverse respiratory health effects. An LBT and AFM were used to evaluate the effects of VOCs on LS (Zhao et al., 2019b). Various VOCs were found to affect surface tension, surface pressure isotherms, and structural transitions in DPPC monolayers. Similar results were observed in animal sourced surfactant (Zhao et al., 2019c).

Smoking and vaping products

Environmental tobacco smoke (ETS) is inhaled by bystanders and has been linked t cancer and asthma in nonsmoking adults. It has also been linked to infections, asthma, and chronic respiratory symptoms in children. Isotherms and morphological information from LBT and AFM show decreases in LS function after ETS exposure (Stenger et al., 2009), likely due to the oxidation of SP-B and diacylation of SP-C.

Vitamin E acetate (VEA) was heavily implicated in an outbreak of thousands of cases of electronic cigarette/vaping associated lung injury. Upon introduction of VEA, LS bilayers were found to have decreased elasticity and increased compressibility, as observed via neutron spin echo spectroscopy and small-angle neutron scattering (DiPasquale et al., 2020). This indicates LS may be inhibited after “softening” induced by VEA.

E-cigarettes have increased in popularity and are often promoted as a safer alternative to conventional smoking. However, increasing evidence has linked e-cigarettes to a variety of diseases and raised concerns over toxic components in their aerosols. E-cigarette aerosols (ECAs) of three different flavors all showed deleterious impacts on LS function, as observed via CDS and AFM (Xu et al., 2022). Nicotine alone had a moderate effect, while flavoring chemicals were observed to have stronger effects. Menthol, a common flavoring agent in ECAs, completely inhibited the monolayer to multilayer transition in LS.

Pathogens

Mycolic acid is associated with pulmonary tuberculosis caused by Mycobacterium tuberculosis. Using an LBT, mycolic acid was found to inhibit a variety of phospholipid monolayers by increasing minimum surface tension (Chimote and Banerjee, 2008). AFM was used to observe surface topology changes.

Bacterial lipopolysaccharide (LPS), also called endotoxin, is present in the cell walls of Gram-negative bacteria and is known to cause local inflammation and system toxicity. LPS was observed by microscopy and compressibility to fluidize phospholipid monolayers (Canadas et al., 2011). Structural collapse at high surface tension was observed via LBT. SP-A was implicated as a scavenger of LPS.

Glucans are structural components of the cell walls of many pathogenic fungi and bacteria. Humans may be exposed to β-D-glucan through the inhalation of organic dusts. β-D-glucan was found to inhibit LS spreading, fluidize LS, and extract lipids from LS as observed by LBT, fluorescence anisotropy, and DSC (Canadas et al., 2022). β-D-glucan was also observed to bind with SP-A.

Plastic particles

Microplastics are widespread global pollutants resulting from the degradation of waste plastic in the environment by various processes. Adsorption of LS phospholipids and proteins onto the surface of microplastic particles was observed by spectroscopy and SEM. Surface pressure changes were investigated with respect to dose. Microplastics were found to promote the production of hydroxyl radical in LS (Shi et al., 2022).

Molecular dynamics simulations have been used to study the interactions 5 types of nanoplastic particles with LS (Li et al., 2022). The time-resolved adsorption of an LS corona was observed for all nanoplastics. Polypropylene and polyvinyl chloride nanoplastics were found to immediately dissolve upon LS adsorption. The effects of aging properties were investigated as well as the leaching of additive bisphenol A. Nanoplastics were observed to perturb LS film stability and cause collapse at high surface tension.

Other

LS function was evaluated after exposure to four representative pollutant nanoparticles: calcium sulfate ($CaSO_4$), carbon (C), silicon dioxide (SiO_2), and hexanediol ($C_6H_{14}O_2$) (Yue et al., 2019). Molecular dynamics simulations were used to study the translocation of each nanoparticle across an LS monolayer during compression (exhalation) and expansion (inhalation) states, as well as order parameter, area per lipid, and surface pressure. Variations with particle size, particle shape, and cholesterol content were also explored. C nanoparticles demonstrated an inability to translocate in either state, as well as stronger

interactions with the monolayer resulting in decreased lipid order and increased surface pressure. $CaSO_4$ interaction was condition dependent and the other two nanoparticle types showed negligible effects.

Per- and polyfluoroalkyl substances (PFAS) are widely used in polymerization processes to produce polishes, paints, and coatings. They are also well-known persistent organic pollutants that bioaccumulate and can cause adverse health effects including thyroid disease, kidney cancer, testicular cancer, liver damage, and various developmental effects. Four salts of PFAS were shown to inhibit LS function (in native porcine LS as measured by a CDS) and induce pro-inflammatory response (in human bronchial epithelial cells) (Sorli et al., 2020).

Lung surfactant toxicology and nanoparticles

Metal based nanoparticles

Airborne nanoparticles composed of metals and metal oxides may be generated from a variety of sources, including manufacturing processes, contamination in the combustion of fossil fuels, activities such as mining, and the weathering of metallic materials.

Engineered gold nanoparticles have been extensively studied for various applications in diagnostics, therapeutics, catalysts, and imaging agents. Gold nanoparticles were found to inhibit LS as observed by CBS (Bakshi et al., 2008), likely due to interactions with LS phospholipids. Alkylated gold nanoparticles were observed via LBT, AFM, and BAM to affect the nucleation, growth, and morphology of condensed domains in DPPC monolayers but not LS monolayers (Bakshi et al., 2008). Coarse-grained molecular dynamics simulations showed the inhibition of LS by gold nanoparticles due to deformation of the monolayer, the formation of pores, and alterations to surface activity (Hossain et al., 2019).

Titanium dioxide is found ubiquitously in pigments, coatings, consumer products, and other applications. A study with micro and nano sized titanium dioxide found that only the nanoparticles inhibited LS function in a PBS (Schleh et al., 2009). In addition, titanium dioxide nanoparticles induced aberrations in LS ultrastructure, *e.g.,* deformed and shrunken lamellar bodies.

Cerium oxide nanoparticles are manufactured for various applications including coatings, polishing agents, and diesel additives. Aerosols of cerium oxide nanoparticles were deposited on LS in an LBT and films were imaged with TEM and SEM (Miguel Diez et al., 2019). The particles showed different effects on surface tension based on delivery method, due to differences in aggregation state.

Zinc oxide nanoparticles are used in industrial applications include paints and sunscreens. Exposure of LS to zinc oxide nanoparticles in a CDS showed inhibition of LS function, whereas zinc ions did not (Larsen et al., 2020). Inhalation of zinc nanoparticles caused shallow breathing in macrophage depleted mice shortly after exposure, validating that inhalation toxicity is related to the interactions with LS.

One study aimed to broadly survey metal-based nanoparticles using the CDS, LBT, and AFM techniques (Yang et al., 2018). Six nanoparticle types were studied, with the potential to inhibit LS ranking as follows: cerium oxide, zinc oxide, titanium dioxide, silver, iron (II, III) oxide, and 78 % zirconium oxide doped cerium oxide. The ranking observed was consistent with previous results *in vitro* and *in vivo*. Imaging implicated that inhibition was driven by aggregation state at the LS film, which in turn was related to physiochemical properties of the nanoparticles.

Mineral nanoparticles

Hydroxyapatite is a form of calcium apatite mineral that is found in geological as well as biological contexts (such as bone and tooth enamel). Hydroxyapatite nanoparticles were found to inhibit LS by protein adsorption onto the particles, as observed by LBT, AFM, and TEM (Fan et al., 2011). Protein depletion led to transitions from large to small phospholipid vesicles, decreasing surface activity.

Aluminosilicate minerals are a large component of many clays and are also used in manufacturing specialty glass as well as fillers for polymer nanocomposites. LS was exposed to halloysite, bentonite and a series of montmorillonite varieties of aluminosilicate nanoparticles in a PBS (Kondej and Sosnowski, 2013). Higher doses were capable of inhibiting LS surface tension and hysteresis, potentially due to the adsorption of LS components. Further study with these materials elucidated the role of hydrophilicity/hydrophobicity (Kondej and Sosnowski, 2016).

Colloidal silica nanoparticles have a variety of applications in industrial and consumer products. Microscopy showed that cellular uptake of silica nanoparticles was inhibited by LS due to nanoparticle-LS interactions (Radiom et al., 2020). Fumed (pyrogenic) silica is another variety of silica used in various applications due to its low density, high surface area, and high viscosity. Fumed silica nanoparticles were found to incorporate into LS monolayers in an LBT and disrupt structure at the interface, inhibiting the function of LS (Guzman et al., 2022).

Polymeric nanoparticles

Polysiloxanes (silicones) are widely used as sealants, adhesives, lubricants, and additives in various industries. AmorSil20 is a hydrophobic nanoparticle with a polyorganosiloxane shell around a polydimethylsiloxane core. LBT and AFM showed AmorSil20 incorporation into LS monolayers, disrupting structure through expansion and fluidization (Harishchandra et al., 2010).

Poly(D,L-lactide-*co*-glycolide) or PLGA is a copolymer approved in various U.S. Food & Drug Administration (FDA) therapeutics due to biodegradability and biocompatibility. Polystyrene (PST) is a thermoplastic used in a wide range of applications. Two varieties of PLGA, P02A and P103E, and PST nanoparticles were studied for their effects on LS via LBT, AFM, and CDS (Valle et al., 2014). Increasing nanoparticle hydrophobicity was associated with increased retention at the LS monolayer and increased inhibition. Another study applied aerosols of carboxyl modified PST nanoparticles to LS in an LBT (Farnoud and Fiegel, 2016), finding that LS function was restored after cycling post-inhibition. Yet another study examined anionic PST with sulfate groups (PSA) and cationic PST with amidine groups (PSC) (Bykov et al., 2022). Despite differences in charge, PSA and PSC had similarly minor effects on LS monolayers as observed via LBT and BAM.

Carbonaceous nanoparticles

A wide variety of carbonaceous nanoparticles have been developed for applications in composite materials, energy storage, semiconductors devices, and other areas. LS was exposed to carbon nanotubes (CNT) and graphite nanoplatelets (GNP) in a CDS (Valle et al., 2015). Dose-dependent inhibition of the LS was observed, as well as perturbation of the structure by adsorbed aggregates using LBT and AFM. Mesoporous carbon nanomaterials were also shown to inhibit LS using CDS (Chen et al., 2017).

Molecular dynamics simulations were used to study the interactions of carbon nanotubes with LS (Yue et al., 2017; Yue et al., 2017). Ultrashort single-walled CNTs were able to rapidly internalize into LS monolayers by self-rotation. Free energy calculations indicate that the CNTs may be difficult to remove and prone to accumulation. Pores were found to open in the LS monolayer due to segregation of lipid components by the CNTs. The translocation of single-walled CNTs across LS membranes was found to be dependent on size and surface patterning.

Lung surfactant toxicology and manufactured products

Industrial products

Polyhexamethylene guanidine (PHMG) is an ingredient that was used in humidifier disinfectant and was implicated in an outbreak of lung injuries with pulmonary fibrosis. CDS, mice, and molecular docking were used to investigate the mechanisms by which PHMG caused fibrosis (Li et al., 2021). PHMG was found to increase LS surface tension and inhibit the expression of SP-B and SP-C while blocking active sites.

Rotenone is a broad-spectrum pesticide used globally in agriculture. Rotenone was found to interact with all LS proteins (SP-A, SP-B, SP-C,

SP-D) at multiple sites via molecular docking simulations (Rajak et al., 2021). Rotenone could potentially impair respiratory function and pathogen defense via the inhibition of LS proteins.

Three industrial chemicals (used in coatings, solvents, and fragrances) known to have acute inhalation toxicity were evaluated for potential LS toxicity. An array of techniques was utilized including CDS, CBS, LBT, Cryo-TEM, and DSC (Da Silva et al., 2021b). Inhibition of LS was related to partial fluidization of condensed phases by insertion between phospholipids, resulting in reduced stability and cohesion. Inhibition was also observed in surface pressure changes and visual transitions.

A series of 26 chemicals which had already been tested for acute inhalation toxicity were investigated for potential effects on LS function (Da Silva et al., 2021c). CDS data was compared to GHS (Globally Harmonized System of Classification and Labeling of Chemicals) and acute toxicity data. The LS bioassay was shown to have 81 % sensitivity and 80 % specificity relative to *in vivo* data. Correlations were not observed with GHS classification.

Consumer products

Nanofilm spray products (NFPs) are typically used for waterproofing of materials by consumers and professionals. After application to a surface, chemical reaction forms a durable and thin hydrophobic film. A particular NFP was withdrawn from the market after showing acute lethality in mice with an unusually steep dose-response relationship. Products with similar structure are still widely available. A capillary surfactometer and mice were used to elucidate the mode of toxic action for an NFP based on a perfluorinated siloxane (Larsen et al., 2014). The NFP inhibited LS function and formed non-covalent interactions with SP-B.

Impregnation products are widely used on materials to seal, repel stains, and improve surface durability. A CDS and mice were used to investigate potential correlation between *in vitro* LS inhibition and *in vivo* inhalation toxicity for a series of 21 impregnation products (Sorli et al., 2018). Correlation was observed in 18 of the 21 products (of which 4 showed no inhibition and no toxicity) while the remaining three products showed false positives for LS inhibition.

A wide variety of consumer products are applied as sprays. A series of 21 spray products, of which eight were cleaning products and 13 were impregnation products, were evaluated for LS toxicity by CDS (Sorli et al., 2022). LS inhibition was observed for two of the cleaning products and 11 of the impregnation products. This may indicate the need for updated regulations surrounding impregnation products.

Medical products

Several inhaled medications were found to have no evidence for inhibition of LS using a CDS (Sorli et al., 2016). This result held even at doses that were orders of magnitude higher than prescribed clinical use.

Synthetic lung surfactant

Early surfactant preparations were sourced from animals either by extracting LS complex with an instilled bronchoalveolar lavage solution, or by directly mincing the removed lungs and washing with saline. Surfactant has also been formulated and prepared using synthetic ingredients. The terminology for this type of surfactant is inconsistent in the literature (Fig. 5.1); hereon we will use the term “synthetic lung surfactant” (SLS) as it appears to be the most widely accepted.

Regardless of origin, LS preparations for both commercial and research purposes have similar equilibrium (adsorption) surface tension values by design (Fig. 5.2). Values generally fall in the 20–25 mN m^{-1} range, as compared to the native human LS at 22–25 mN m^{-1}. (Zuo et al., 2008).

Design and formulation of synthetic surfactants

There are a variety of SLS formulations reported in the literature, each with a different composition of lipid and protein ingredients (Table 5.1). These formulations are designed with the goal of emulating the biophysical properties of animal surfactants while remaining feasible to manufacture.

Non-protein ingredients in synthetic lung surfactant

DPPC is the most abundant phospholipid in native mammalian LS. Its saturated chains allow optimal close packing at maximum compression. DPPC undergoes a melt transition above 41 °C, though this point is increased in dehydrated states (*e.g.,* during lamellar body formation). POPC is another example of a phosphatidylcholine used in SLS. Anionic phosphatidylglycerols (*e.g.,* DPPG, POPG) are also found in LS and are thought to establish interactions with cationic proteins SP-B and SP-C. SLS formulations that include surfactant proteins include some PG to ensure that the proteins adopt proper conformations. Palmitic acid, which has a saturated chain, is present in some formulations to provide additional stability to close packing states. PA and higher amounts of DPPC may promote SLS structure in formulations that lack SP-B. (Perez-Gil, 2022).

While cholesterol and other neutral lipids are present in native LS, the necessity of cholesterol in SLS is still debated. While cholesterol provides fluidity to cell membranes and native LS, cholesterol is shown to inhibit surface activity in simple lipid systems and elevated cholesterol levels are found in the deteriorated LS of RDS patients. Cholesterol is absent from most SLS formulations or deliberately removed from *ex vivo* preparations. Some recent work challenges this view, and some formulations choose to include cholesterol, such as the Forbes group of King’s College London (F-KCL in Table 5.1). (Perez-Gil, 2022; Hassoun et al., 2018; Mingarro et al., 2008).

While not a common ingredient in SLS formulations, cetyl alcohol (a fatty alcohol) and tylaxopol (a liquid polymer alcohol) are notably included in Exosurf. They act as spreading agents, as Exosurf does not contain any surfactant proteins or protein analogs. Both cetyl alcohol and tylaxopol have been used as surfactants in other medical treatments and consumer products. (Mingarro et al., 2008).

Protein ingredients in synthetic lung surfactant

The major bottleneck in LS production for clinical or research use is obtaining adequate amounts of functional surfactant protein. Resource constraints and concerns such as product consistency or pathogens have incentivized the synthesis of alternatives to *ex vivo* SP-B and SP-C. The two dominant approaches are recombinant protein and protein analogs. (Perez-Gil, 2022).

Recombinant processes use a vector and host system (typically mammalian or bacterial cells) to produce large quantities of a desired protein. Genes are inserted into the host DNA to form recombinant DNA, which are then expressed to produce the desire protein. Methods have been developed for recombinant SP-B and SP-C production, and some SLS formulations have included recombinant protein (*e.g.,* Venticute). (Rosano and Ceccarelli, 2014; Chu and Robinson, 2001; Korst et al., 1995; Lukovic et al., 2006).

Full-length SP-B synthesis has been accomplished, but the tertiary structure and behaviors characteristic to native SP-B was not replicated successfully. Due to these challenges, efforts have focused on developing simpler analogs to SP-B. These include Mini-B (a 34-residue peptide corresponding to the first and last helices of SP-B), Super Mini-B (Mini-B with an added 7-residue hydrophobic segment), and sinapultide or KL4 (a 21-residue peptide inspired by the C-terminal portion of SP-B). Full-length SP-C has been synthesized but the replicates tend to aggregate and show poor surface activity. This has led to the replacement of segments to create hybrid peptides and more extensive modifications as seen in SP-CLeu and SP-CLKS. Optimization of SP-C analog properties is ongoing with a wide variety of specific insertions or deletions under

consideration. (Johansson and Curstedt, 2019; Walther et al., 2019).

Recent advances for synthetic surfactants

Two clinical trials have been conducted for a synthetic lung surfactant in the past decade, both for CHF5633. Developed by Chiesi Farmaceutici in Italy, CHF5633 contains 0.2 % Mini-B (SP-B analog) and 1.5 % SP-C33Leu (SP-C analog) in a 1:1 mixture of DPPC:POPG. The 2017 trial showed promising efficacy at two well-tolerated doses. The 2020 multicenter, double-blind, randomized, controlled trial showed similar efficacy and safety of CHF5633 as compared to Curosurf. Minisurf, developed by Molecular Express Inc in the USA, is another new SLS formulation with 3 % Super Mini-B in a 5:3:2 mixture of DPPC:POPC:POPG. Minisurf is currently in a preclinical stage. Very recent work has led to the synthesis of a "combo peptide" that mimics features of both SP-B and SP-C, promoting both intermembrane and intramembrane activity. (Walther et al., 2019; Sweet et al., 2017; Ramanathan et al., 2020; Basabe-Burgos et al., 2021).

In addition to synthetic peptides, synthetic lipids have been developed and investigated for use in SLS. DEPN-8 and PG-1 are example analogs for DPPC and POPG, respectively. Both are designed to be resistant to phospholipase degradation. Phospholipase activity is elevated during inflammatory conditions associated with acute lung injury (ALI) and adult RDS. The subsequent loss of glycerophospholipids and generation of reaction products lysophosphatidylcholine.

(LPC) and free fatty acids lead to the inhibition of LS activity. SLS formulations that include both synthetic proteins and synthetic lipids can deliver exceptional surface activity while resisting inactivation. (Notter et al., 2007; Notter et al., 2016).

Advantages and prospects of synthetic surfactants

Synthetic lung surfactants have many potential advantages over traditional *ex vivo* surfactants:

- Supply: With the development and scale-up of recombinant or analog protein production, SLS will face fewer supply constraints than *ex vivo* surfactant.
- Time: As supply chain infrastructure develops, SLS production can provide faster turnaround than *ex vivo* surfactant (which requires animals to gestate and mature).
- Cost: The synthesis and assembly of select components can be value engineered to reduce cost beyond what is possible with sourcing from animals.
- Quality: Native LS composition can vary at both species and individual levels. Engineering controls can ensure SLS product consistency to a degree that may not be feasible with *ex vivo* surfactant.
- Safety: With *ex vivo* surfactant, the risk for pathogen transfer from the animal is difficult to eliminate. The use of synthetic ingredients eliminates this risk.
- Ethics: Transition to SLS production would decrease dependence on animals, with benefits for both animal welfare and environmental footprint.
- Customization: SLS formulations can be tailored to treat specific conditions or to adapt to specific patient characteristics.

While there are challenges facing SLS development including market incumbents, high development cost, and barriers to approval, the potential advantages make a strong case for shifting to SLS in clinical and research settings. (Perez-Gil, 2022; Mingarro et al., 2008; Willson and Notter, 2011; Kim and Won, 2018).

Despite these advantages, the fraction of LS related research that mentions SLS remains low (Fig. 5.3). While the proportion has gone up slightly in recent years and the total body of LS research is growing, we make the case that synthetic lung surfactants have the potential to outcompete their animal-derived counterparts. SLS also has a relatively unexplored potential as an inhalation toxicology model. Inhibition of SLS may become an endpoint for hazard identification in risk assessment, predictive toxicology, or the screening of chemicals and pharmaceuticals.

The major bottleneck for SLS remains the development and manufacture of humanized surfactant protein analogs. Market incentive may be found in the treatment of adult RDS, which is larger in scale than neonatal RDS. Improvement of aerosolized delivery techniques and possible efficacy in early-stage prevention may further incentivize SLS development. (Perez-Gil, 2022; Kim and Won, 2018).

Conclusions

Lung surfactant (LS) is a mixture of lipids and proteins in the distal airspaces that plays important roles in biophysical and biochemical functions of the lung. These include facilitating gas exchange, stabilizing alveolar structure, particle biotransformation, particle clearance, and innate immunity. The phospholipids, neutral lipids, surfactant proteins, and microstructures (lamellar bodies, tubular myelin, and small vesicles) of LS drive these functions. Dysfunction in surfactant metabolism or inhibition of surfactant by various endogenous or exogenous substances can result in impaired lung function and numerous pathologies.

Research on LS has conventionally focused on surfactant replacement therapy in clinical settings to treat respiratory distress syndrome and other conditions. More recent research has explored LS as a toxicological model to investigate potentially harmful substances. A narrative review was conducted of these studies, analyzing the methods used and the categories of toxicants studied. The trajectory of this area of research demonstrates the utility and feasibility of LS as a biophysical assay for inhalation toxicology.

Synthetic lung surfactants have been developed and evaluated as an alternative to animal derived surfactant. Synthetic lung surfactants have seen several recent advances and pose numerous advantages related to production, utility, and ethics of use. More research is needed to improve component synthesis, formulations, and manufacturing methods. These improvements would empower the wider use of synthetic lung surfactants in clinical and toxicological contexts.

Declaration of Competing Interest

The authors declare that they have no known competing financial interests or personal relationships that could have appeared to influence the work reported in this paper.

Data availability

Data will be made available on request.

References

Ainsworth, S.B., 2005. Pathophysiology of neonatal respiratory distress syndrome: implications for early treatment strategies. Treat Respir Med 4 (6), 423–437.
Alonso, C., Waring, A., Zasadzinski, J.A., 2005. Keeping lung surfactant where it belongs: protein regulation of two-dimensional viscosity. Biophys J 89 (1), 266–273.
Anseth, J.W., Goffin, A.J., Fuller, G.G., Ghio, A.J., Kao, P.N., Upadhyay, D., 2005. Lung surfactant gelation induced by epithelial cells exposed to air pollution or oxidative stress. Am J Respir Cell Mol Biol 33 (2), 161–168.
Astashkina, A., Mann, B., Grainger, D.W., 2012. A critical evaluation of in vitro cell culture models for high-throughput drug screening and toxicity. Pharmacol Ther 134 (1), 82–106.
Autilio, C., Perez-Gil, J., 2019. Understanding the principle biophysics concepts of pulmonary surfactant in health and disease. Arch Dis Child Fetal Neonatal Ed 104 (4), F443. F451.
Avery, M.E., Mead, J., 1959. **Surface properties in relation to atelectasis and hyaline membrane disease**. *AMA J Dis.* Child 97(5, Part 1):517–523.
Bakshi, M.S., Zhao, L., Smith, R., Possmayer, F., Petersen, N.O., 2008. Metal nanoparticle pollutants interfere with pulmonary surfactant function in vitro. Biophys J 94 (3), 855–868.
Basabe-Burgos, O., Landreh, M., Rising, A., Curstedt, T., Jan, J., 2021. Treatment of Respiratory Distress Syndrome with Single Recombinant Polypeptides that Combine Features of SP-B and SP-C. ACS Chem Biol 16 (12), 2864–2873.

Beers, M.F., Fisher, A.B., 1992. Surfactant protein C: a review of its unique properties and metabolism. Am J Physiol 263 (2 Pt 1), L151. L160.
Bernhard, W., 2016. Lung surfactant: Function and composition in the context of development and respiratory physiology. Ann Anat 208, 146–150.
Blodgett, K.B., 2002. Monomolecular Films of Fatty Acids on Glass. Journal of the American Chemical Society 56 (2), 495.
Braun, A., Stenger, P.C., Warriner, H.E., Zasadzinski, J.A., Lu, K.W., Taeusch, H.W., 2007. A freeze-fracture transmission electron microscopy and small angle x-ray diffraction study of the effects of albumin, serum, and polymers on clinical lung surfactant microstructure. Biophys J 93 (1), 123–139.
Bykov, A., Milyaeva, O., Akentiev, A., Panaeva, M., Isakov, N., Miller, R., Noskov, B., 2022. Impact of Polymer Nanoparticles on DPPC Monolayer Properties. Colloids and Interfaces 6 (2).
Canadas, O., Keough, K.M., Casals, C., 2011. Bacterial lipopolysaccharide promotes destabilization of lung surfactant-like films. Biophys J 100 (1), 108–116.
Canadas, O., Saenz, A., de Lorenzo, A., Casals, C., 2022. Pulmonary surfactant inactivation by beta-D-glucan and protective role of surfactant protein A. Colloids Surf B Biointerfaces 210, 112237.
Cao, Y., Zhao, Q., Geng, Y., Li, Y., Huang, J., Tian, S., Ning, P., 2021. Interfacial interaction between benzo[a]pyrene and pulmonary surfactant: Adverse effects on lung health. Environ Pollut 287, 117669.
Castillo-Sanchez, J.C., Cruz, A., Perez-Gil, J., 2021. Structural hallmarks of lung surfactant: Lipid-protein interactions, membrane structure and future challenges. Arch Biochem Biophys 703, 108850.
Chakraborty, M., Kotecha, S., 2013. Pulmonary surfactant in newborn infants and children. Breathe 9 (6), 476–488.
Chen, Y., Yang, Y., Xu, B., Wang, S., Li, B., Ma, J., Gao, J., Zuo, Y.Y., Liu, S., 2017. Mesoporous carbon nanomaterials induced pulmonary surfactant inhibition, cytotoxicity, inflammation and lung fibrosis. J Environ Sci (China) 62, 100–114.
Chimote, G., Banerjee, R., 2008. Effect of mycolic acid on surface activity of binary surfactant lipid monolayers. J Colloid Interface Sci 328 (2), 288–298.
Chu, L., Robinson, D.K., 2001. Industrial choices for protein production by large-scale cell culture. Current Opinion in Biotechnology 12 (2), 180–187.
Clark, D.A., Nieman, G.F., Thompson, J.E., Paskanik, A.M., Rokhar, J.E., Bredenberg, C. E., 1987. Surfactant displacement by meconium free fatty acids: An alternative explanation for atelectasis in meconium aspiration syndrome. The Journal of Pediatrics 110 (5), 765–770.
Crouch, E.C., 2000. Surfactant protein-D and pulmonary host defense. Respir Res 1 (2), 93–108.
Crouch EC: **Structure, biologic properties, and expression of surfactant protein D (SP-D)**. *Biochimica et Biophysica Acta (BBA) - Molecular Basis of Disease* 1998, **1408** (2-3):278-289.
Da Silva, E., Autilio, C., Hougaard, K.S., Baun, A., Cruz, A., Perez-Gil, J., Sorli, J.B., 2021a. Molecular and biophysical basis for the disruption of lung surfactant function by chemicals. Biochim Biophys Acta Biomembr 1863 (1), 183499.
Da Silva, E., Hickey, C., Ellis, G., Hougaard, K.S., Sorli, J.B., 2021b. In vitro prediction of clinical signs of respiratory toxicity in rats following inhalation exposure. Curr Res Toxicol 2, 204–209.
Da Silva, E., Vogel, U., Hougaard, K.S., Perez-Gil, J., Zuo, Y.Y., Sorli, J.B., 2021c. An adverse outcome pathway for lung surfactant function inhibition leading to decreased lung function. Curr Res Toxicol 2, 225–236.
Demetzos, C., 2008. Differential Scanning Calorimetry (DSC): a tool to study the thermal behavior of lipid bilayers and liposomal stability. J Liposome Res 18 (3), 159–173.
DiPasquale, M., Gbadamosi, O., Nguyen, M.H.L., Castillo, S.R., Rickeard, B.W., Kelley, E. G., Nagao, M., Marquardt, D., 2020. A Mechanical Mechanism for Vitamin E Acetate in E-cigarette/Vaping-Associated Lung Injury. Chem Res Toxicol 33 (9), 2432–2440.
Dwivedi M, Sachan AK, Galla H-J: **Interaction of Nanoparticles with Lipid Monolayers and Lung Surfactant Films**. In: *Measuring Biological Impacts of Nanomaterials*. 2014: 109-133.
Eggleton, P., Reid, K.B.M., 1999. Lung surfactant proteins involved in innate immunity. Current Opinion in Immunology 11 (1), 28–33.
Ellenbroek, B., Youn, J., 2016. Rodent models in neuroscience research: is it a rat race? Dis Model Mech 9 (10), 1079–1087.
Enhorning, G., 1977. Pulsating bubble technique for evaluating pulmonary surfactant. J Appl Physiol Respir Environ Exerc Physiol 43 (2), 198–203.
Enhorning, G., 2001. Pulmonary surfactant function studied with the pulsating bubble surfactometer (PBS) and the capillary surfactometer (CS). Comparative Biochemistry and Physiology Part A: Molecular & Integrative Physiology 129 (1), 221–226.
Fan, Q., Wang, Y.E., Zhao, X., Loo, J.S., Zuo, Y.Y., 2011. Adverse biophysical effects of hydroxyapatite nanoparticles on natural pulmonary surfactant. ACS Nano 5 (8), 6410–6416.
Fang, Q., Zhao, Q., Chai, X., Li, Y., Tian, S., 2020. Interaction of industrial smelting soot particles with pulmonary surfactant: Pulmonary toxicity of heavy metal-rich particles. Chemosphere 246, 125702.
Farnoud, A.M., Fiegel, J., 2016. Calf Lung Surfactant Recovers Surface Functionality After Exposure to Aerosols Containing Polymeric Particles. J Aerosol Med Pulm Drug Deliv 29 (1), 10–23.
Fasske, E., Morgenroth, K., 1983. Experimental bleomycin lung in mice. A contribution to the pathogenesis of pulmonary fibrosis. Lung 161 (3), 133–146.
Goerke J: **Pulmonary surfactant: functions and molecular composition**. *Biochimica et Biophysica Acta (BBA) - Molecular Basis of Disease* 1998, **1408** (2-3):79-89.
Gradoń, L., Podgórski, A., 1989. Hydrodynamical model of pulmonary clearance. Chemical Engineering Science 44 (3), 741–749.
Guzmán, E., 2022. Fluid Films as Models for Understanding the Impact of Inhaled Particles in Lung Surfactant Layers. Coatings 12 (2).
Guzmán E, Santini E, Ferrari M, Liggieri L, Ravera F: **Evaluation of the impact of carbonaceous particles in the mechanical performance of lipid Langmuir monolayers**. *Colloids and Surfaces A: Physicochemical and Engineering Aspects* 2022, **634**.
Guzman, E., Santini, E., Ferrari, M., Liggieri, L., Ravera, F., 2022. Evaluating the Impact of Hydrophobic Silicon Dioxide in the Interfacial Properties of Lung Surfactant Films. Environ Sci Technol 56 (11), 7308–7318.
Halliday, H.L., 2017. The fascinating story of surfactant. J Paediatr Child Health 53 (4), 327–332.
Han, S., Mallampalli, R.K., 2015. The Role of Surfactant in Lung Disease and Host Defense against Pulmonary Infections. Ann Am Thorac Soc 12 (5), 765–774.
Harishchandra, R.K., Saleem, M., Galla, H.J., 2010. Nanoparticle interaction with model lung surfactant monolayers. J R Soc Interface 7 (Suppl 1), S15–S26.
Hartl, D., Griese, M., 2006. Surfactant protein D in human lung diseases. Eur J Clin Invest 36 (6), 423–435.
Hassoun, M., Royall, P.G., Parry, M., Harvey, R.D., Forbes, B., 2018. Design and development of a biorelevant simulated human lung fluid. J Drug Deliv Sci Technol 47, 485–491.
Hawgood S, Derrick M, Poulain F: **Structure and properties of surfactant protein B**. *Biochimica et Biophysica Acta (BBA) - Molecular Basis of Disease* 1998, **1408** (2-3):150-160.
Hite, R.D., Seeds, M.C., Jacinto, R.B., Grier, B.L., Waite, B.M., Bass, D.A., 2005. Lysophospholipid and fatty acid inhibition of pulmonary surfactant: non-enzymatic models of phospholipase A2 surfactant hydrolysis. Biochim Biophys Acta 1720 (1–2), 14–21.
Holm, B.A., Enhorning, G., Notter, R.H., 1988. A biophysical mechanism by which plasma proteins inhibit lung surfactant activity. Chemistry and Physics of Lipids 49 (1–2), 49–55.
Horowitz, A.D., Baatz, J.E., Whitsett, J.A., 1993. Lipid effects on aggregation of pulmonary surfactant protein SP-C studied by fluorescence energy transfer. Biochemistry 32 (37), 9513–9523.
Hossain, S.I., Gandhi, N.S., Hughes, Z.E., Gu, Y.T., Saha, S.C., 2019. Molecular insights on the interference of simplified lung surfactant models by gold nanoparticle pollutants. Biochim Biophys Acta Biomembr 1861 (8), 1458–1467.
Hu, Q., Bai, X., Hu, G., Zuo, Y.Y., 2017. Unveiling the Molecular Structure of Pulmonary Surfactant Corona on Nanoparticles. ACS Nano 11 (7), 6832–6842.
Hu, J., Li, X., Li, M., Shang, Y., He, Y., Liu, H., 2020. Real-time monitoring of the effect of carbon nanoparticles on the surface behavior of DPPC/DPPG Langmuir monolayer. Colloids Surf B Biointerfaces 190, 110922.
Jain, A.K., Singh, D., Dubey, K., Maurya, R., Mittal, S., Pandey, A.K., 2018. Models and Methods for In Vitro Toxicity. In Vitro Toxicology. 45–65.
Johansson, J., Curstedt, T., 2019. Synthetic surfactants with SP-B and SP-C analogues to enable worldwide treatment of neonatal respiratory distress syndrome and other lung diseases. J Intern Med 285 (2), 165–186.
Johansson J: **Structure and properties of surfactant protein C**. *Biochimica et Biophysica Acta (BBA) - Molecular Basis of Disease* 1998, **1408** (2-3):161-172.
Kanishtha, T., Banerjee, R., Venkataraman, C., 2006. Effect of particle emissions from biofuel combustion on surface activity of model and therapeutic pulmonary surfactants. Environ Toxicol Pharmacol 22 (3), 325–333.
Kapralov, A.A., Feng, W.H., Amoscato, A.A., Yanamala, N., Balasubramanian, K., Winnica, D.E., Kisin, E.R., Kotchey, G.P., Gou, P., Sparvero, L.J., et al., 2012. Adsorption of surfactant lipids by single-walled carbon nanotubes in mouse lung upon pharyngeal aspiration. ACS Nano 6 (5), 4147–4156.
Khabib, M.N.H., Sivasanku, Y., Lee, H.B., Kumar, S., Kue, C.S., 2022. Alternative animal models in predictive toxicology. Toxicology 465, 153053.
Khubchandani, K.R., Snyder, J.M., 2001. Surfactant protein A (SP-A): the alveolus and beyond. FASEB J 15 (1), 59–69.
Kim, H.C., Won, Y.Y., 2018. Clinical, technological, and economic issues associated with developing new lung surfactant therapeutics. Biotechnol Adv 36 (4), 1185–1193.
King, S.D., Chen, S.Y., 2020. Recent progress on surfactant protein A: cellular function in lung and kidney disease development. Am J Physiol Cell Physiol 319 (2), C316. C320.
Kingma, P.S., Whitsett, J.A., 2006. In defense of the lung: surfactant protein A and surfactant protein D. Curr Opin Pharmacol 6 (3), 277–283.
Kinter, L.B., DeHaven, R., Johnson, D.K., DeGeorge, J.J., 2021. A Brief History of Use of Animals in Biomedical Research and Perspective on Non-Animal Alternatives. ILAR J.
Kondej, D., Sosnowski, T.R., 2013. Alteration of biophysical activity of pulmonary surfactant by aluminosilicate nanoparticles. Inhal Toxicol 25 (2), 77–83.
Kondej, D., Sosnowski, T.R., 2016. Effect of clay nanoparticles on model lung surfactant: a potential marker of hazard from nanoaerosol inhalation. Environ Sci Pollut Res Int 23 (5), 4660–4669.
Korst, R.J., Bewig, B., Crystal, R.G., 1995. In vitro and in vivo transfer and expression of human surfactant SP-A- and SP-B-associated protein cDNAs mediated by replication-deficient, recombinant adenoviral vectors. Hum Gene Ther 6 (3), 277–287.
Langmuir I: **The Constitution and Fundamental Properties of Solids and Liquids. Ii. Liquids.1**. *Journal of the American Chemical Society* 2002, **39** (9):1848-1906.
Larsen, S.T., Dallot, C., Larsen, S.W., Rose, F., Poulsen, S.S., Norgaard, A.W., Hansen, J. S., Sorli, J.B., Nielsen, G.D., Foged, C., 2014. Mechanism of action of lung damage caused by a nanofilm spray product. Toxicol Sci 140 (2), 436–444.
Larsen, S.T., Da Silva, E., Hansen, J.S., Jensen, A.C.O., Koponen, I.K., Sorli, J.B., 2020. Acute Inhalation Toxicity After Inhalation of ZnO Nanoparticles: Lung Surfactant Function Inhibition In Vitro Correlates With Reduced Tidal Volume in Mice. Int J Toxicol 39 (4), 321–327.

Larsson, M., Nylander, T., Keough, K.M., Nag, K., 2006. An X-ray diffraction study of alterations in bovine lung surfactant bilayer structures induced by albumin. Chem Phys Lipids 144 (2), 137–145.
Lesur, O., Veldhuizen, R.A., Whitsett, J.A., Hull, W.M., Possmayer, F., Cantin, A., Begin, R., 1993. Surfactant-associated proteins (SP-A, SP-B) are increased proportionally to alveolar phospholipids in sheep silicosis. Lung 171 (2), 63–74.
Li, L., Xu, Y., Li, S., Zhang, X., Feng, H., Dai, Y., Zhao, J., Yue, T., 2022. Molecular modeling of nanoplastic transformations in alveolar fluid and impacts on the lung surfactant film. J Hazard Mater 427, 127872.
Li, X., Zhang, J., Du, C., Jiang, Y., Zhang, W., Wang, S., Zhu, X., Gao, J., Zhang, X., Ren, D., et al., 2021. Polyhexamethylene guanidine aerosol triggers pulmonary fibrosis concomitant with elevated surface tension via inhibiting pulmonary surfactant. J Hazard Mater 420, 126642.
Lu, K.W., Perez-Gil, J., Taeusch, H., 2009. Kinematic viscosity of therapeutic pulmonary surfactants with added polymers. Biochim Biophys Acta 1788 (3), 632–637.
Lukovic, D., Plasencia, I., Taberner, F.J., Salgado, J., Calvete, J.J., Perez-Gil, J., Mingarro, I., 2006. Production and characterisation of recombinant forms of human pulmonary surfactant protein C (SP-C): Structure and surface activity. Biochim Biophys Acta 1758 (4), 509–518.
Malcharek, S., Hinz, A., Hilterhaus, L., Galla, H.J., 2005. Multilayer structures in lipid monolayer films containing surfactant protein C: effects of cholesterol and POPE. Biophys J 88 (4), 2638–2649.
Martinez-Calle, M., Parra-Ortiz, E., Cruz, A., Olmeda, B., Perez-Gil, J., 2021. Towards the Molecular Mechanism of Pulmonary Surfactant Protein SP-B: At the Crossroad of Membrane Permeability and Interfacial Lipid Transfer. J Mol Biol 433 (3), 166749.
Mason, R.J., Greene, K., Voelker, D.R., 1998. Surfactant protein A and surfactant protein D in health and disease. Am J Physiol 275 (1), L1–L.
Miguel Diez, M., Buckley, A., Tetley, T.D., Smith, R., 2019. The method of depositing CeO2 nanoparticles onto a DPPC monolayer affects surface tension behaviour. NanoImpact 16.
Mingarro, I., Lukovic, D., Vilar, M., Perez-Gil, J., 2008. Synthetic pulmonary surfactant preparations: new developments and future trends. Curr Med Chem 15 (4), 393–403.
Mulugeta, S., Beers, M.F., 2006. Surfactant protein C: its unique properties and emerging immunomodulatory role in the lung. Microbes Infect 8 (8), 2317–2323.
Neergaard, K., 1929. Neue Auffassungen über einen Grundbegriff der Atemmechanik. Zeitschrift für Die Gesamte Experimentelle Medizin 66 (1), 373–394.
Nkadi, P.O., Merritt, T.A., Pillers, D.A., 2009. An overview of pulmonary surfactant in the neonate: genetics, metabolism, and the role of surfactant in health and disease. Mol Genet Metab 97 (2), 95–101.
Notter RH, Wang ZH, Schwan AL, Wang ZY, Davy JA, Waring AJ, Walther F, Gordon LM: **Synthetic lung surfactant and use thereof**. In. Edited by USPTO. USA; 2016.
Notter, R.H., Schwan, A.L., Wang, Z., Waring, A.J., 2007. Novel phospholipase-resistant lipid/peptide synthetic lung surfactants. Mini Rev Med Chem 7 (9), 932–944.
Oliveira Jr., O.N., Caseli, L., Ariga, K., 2022. The Past and the Future of Langmuir and Langmuir-Blodgett Films. Chem Rev 122 (6), 6459–6513.
Parra, E., Perez-Gil, J., 2015. Composition, structure and mechanical properties define performance of pulmonary surfactant membranes and films. Chem Phys Lipids 185, 153–175.
Pattle, R.E., 1955. Properties, function and origin of the alveolar lining layer. Nature 175 (4469), 1125–1126.
Perez-Gil, J., 2022. A recipe for a good clinical pulmonary surfactant. Biomed J.
Pioselli, B., Salomone, F., Mazzola, G., Amidani, D., Sgarbi, E., Amadei, F., Murgia, X., Catinella, S., Villetti, G., De Luca, D., et al., 2022. Pulmonary Surfactant: A Unique Biomaterial with Life-saving Therapeutic Applications. Curr Med Chem 29 (3), 526–590.
Postle, A.D., Mander, A., Reid, K.B., Wang, J.Y., Wright, S.M., Moustaki, M., Warner, J. O., 1999. Deficient hydrophilic lung surfactant proteins A and D with normal surfactant phospholipid molecular species in cystic fibrosis. Am J Respir Cell Mol Biol 20 (1), 90–98.
Poulain, F.R., Allen, L., Williams, M.C., Hamilton, R.L., Hawgood, S., 1992. Effects of surfactant apolipoproteins on liposome structure: implications for tubular myelin formation. Am J Physiol 262 (6 Pt 1), L730–L930.
Radiom, M., Sarkis, M., Brookes, O., Oikonomou, E.K., Baeza-Squiban, A., Berret, J.F., 2020. Pulmonary surfactant inhibition of nanoparticle uptake by alveolar epithelial cells. Sci Rep 10 (1), 19436.
Raesch, S.S., Tenzer, S., Storck, W., Rurainski, A., Selzer, D., Ruge, C.A., Perez-Gil, J., Schaefer, U.F., Lehr, C.M., 2015. Proteomic and Lipidomic Analysis of Nanoparticle Corona upon Contact with Lung Surfactant Reveals Differences in Protein, but Not Lipid Composition. ACS Nano 9 (12), 11872–11885.
Rajak, P., Roy, S., Pal, A.K., Paramanik, M., Dutta, M., Podder, S., Sarkar, S., Ganguly, A., Mandi, M., Dutta, A., et al., 2021. In silico study reveals binding potential of rotenone at multiple sites of pulmonary surfactant proteins: A matter of concern. Curr Res Toxicol 2, 411–423.
Ramanathan, R., Biniwale, M., Sekar, K., Hanna, N., Golombek, S., Bhatia, J., Naylor, M., Fabbri, L., Varoli, G., Santoro, D., et al., 2020. Synthetic Surfactant CHF5633 Compared with Poractant Alfa in the Treatment of Neonatal Respiratory Distress Syndrome: A Multicenter, Double-Blind, Randomized, Controlled Clinical Trial. J Pediatr 225 (90–96), e91.
Rampado, R., Crotti, S., Caliceti, P., Pucciarelli, S., Agostini, M., 2020. Recent Advances in Understanding the Protein Corona of Nanoparticles and in the Formulation of "Stealthy" Nanomaterials. Front Bioeng Biotechnol 8, 166.
Ravera, F., Miller, R., Zuo, Y.Y., Noskov, B.A., Bykov, A.G., Kovalchuk, V.I., Loglio, G., Javadi, A., Liggieri, L., 2021. Methods and models to investigate the physicochemical functionality of pulmonary surfactant. Current Opinion in Colloid & Interface Science 55.
Rosano, G.L., Ceccarelli, E.A., 2014. Recombinant protein expression in Escherichia coli: advances and challenges. Front Microbiol 5, 172.
Rubin, B.K., Tomkiewicz, R.P., Patrinos, M.E., Easa, D., 1996. The surface and transport properties of meconium and reconstituted meconium solutions. Pediatr Res 40 (6), 834–838.
Saenz, A., Canadas, O., Bagatolli, L.A., Sanchez-Barbero, F., Johnson, M.E., Casals, C., 2007. Effect of surfactant protein A on the physical properties and surface activity of KL4-surfactant. Biophys J 92 (2), 482–492.
Scarpelli, E., 1995. R.E. Pattle and the discovery of lung surfactant. Am J Perinatol 12 (5), 377–378.
Schleh, C., Muhlfeld, C., Pulskamp, K., Schmiedl, A., Nassimi, M., Lauenstein, H.D., Braun, A., Krug, N., Erpenbeck, V.J., Hohlfeld, J.M., 2009. The effect of titanium dioxide nanoparticles on pulmonary surfactant function and ultrastructure. Respir Res 10, 90.
Schurch, S., Bachofen, H., Goerke, J., Possmayer, F., 1989. A captive bubble method reproduces the in situ behavior of lung surfactant monolayers. J Appl Physiol (1985) 67 (6), 2389–2396.
Schürch, S., Green, F.H.Y., Bachofen, H., 1998. **Formation and structure of surface films: captive bubble surfactometry**. *Biochimica et Biophysica Acta (BBA)*. - Molecular Basis of Disease 1408 (2–3), 180–202.
Shi, W., Cao, Y., Chai, X., Zhao, Q., Geng, Y., Liu, D., Tian, S., 2022. Potential health risks of the interaction of microplastics and lung surfactant. J Hazard Mater 429, 128109.
Shibasaki, M., Hashimoto, K., Okamoto, M., Hayashi, Y., Imaizumi, K., Hashimoto, N., Ozaki, N., Yokoi, T., Takagi, K., Hasegawa, Y., et al., 2009. Up-regulation of surfactant protein production in a mouse model of secondary pulmonary alveolar proteinosis. Am J Respir Cell Mol Biol 40 (5), 536–542.
Smith, P.B., Ambalavanan, N., Li, L., Cotten, C.M., Laughon, M., Walsh, M.C., Das, A., Bell, E.F., Carlo, W.A., Stoll, B.J., et al., 2012. Approach to infants born at 22 to 24 weeks' gestation: relationship to outcomes of more-mature infants. Pediatrics 129 (6), e1508–e1516.
Sorli, J.B., Da Silva, E., Backman, P., Levin, M., Thomsen, B.L., Koponen, I.K., Larsen, S. T., 2016. A Proposed In Vitro Method to Assess Effects of Inhaled Particles on Lung Surfactant Function. Am J Respir Cell Mol Biol 54 (3), 306–311.
Sorli, J.B., Huang, Y., Da Silva, E., Hansen, J.S., Zuo, Y.Y., Frederiksen, M., Norgaard, A. W., Ebbehoj, N.E., Larsen, S.T., Hougaard, K.S., 2018. Prediction of acute inhalation toxicity using in vitro lung surfactant inhibition. ALTEX 35 (1), 26–36.
Sorli, J.B., Lag, M., Ekeren, L., Perez-Gil, J., Haug, L.S., Da Silva, E., Matrod, M.N., Gutzkow, K.B., Lindeman, B., 2020. Per- and polyfluoroalkyl substances (PFASs) modify lung surfactant function and pro-inflammatory responses in human bronchial epithelial cells. Toxicol In Vitro 62, 104656.
Sorli, J.B., Sengupta, S., Jensen, A.C.O., Nikiforov, V., Clausen, P.A., Hougaard, K.S., Hojriis, S., Frederiksen, M., Hadrup, N., 2022. Risk assessment of consumer spray products using in vitro lung surfactant function inhibition, exposure modelling and chemical analysis. Food Chem Toxicol 164, 112999.
Sosnowski, T.R., 2018. Particles on the lung surface - physicochemical and hydrodynamic effects. Current Opinion in Colloid & Interface Science 36, 1–9.
Sosnowski, T.R., Kolinski, M., Gradon, L., 2011. Interactions of benzo[a]pyrene and diesel exhaust particulate matter with the lung surfactant system. Ann Occup Hyg 55 (3), 329–338.
Spink CH: **Differential Scanning Calorimetry**. In: *Biophysical Tools for Biologists, Volume One: In Vitro Techniques.* 2008: 115-141.
Steiner, R.F., 2002. Fluorescence Anisotropy: Theory and Applications. Topics in Fluorescence Spectroscopy. 1–52.
Stenger, P.C., Wu, G., Miller, C.E., Chi, E.Y., Frey, S.L., Lee, K.Y., Majewski, J., Kjaer, K., Zasadzinski, J.A., 2009. X-ray diffraction and reflectivity validation of the depletion attraction in the competitive adsorption of lung surfactant and albumin. Biophys J 97 (3), 777–786.
Sun, B., Curstedt, T., Robertson, B., 1993. Surfactant inhibition in experimental meconium aspiration. Acta Paediatr 82 (2), 182–189.
Sweet, D.G., Turner, M.A., Stranak, Z., Plavka, R., Clarke, P., Stenson, B.J., Singer, D., Goelz, R., Fabbri, L., Varoli, G., et al., 2017. A first-in-human clinical study of a new SP-B and SP-C enriched synthetic surfactant (CHF5633) in preterm babies with respiratory distress syndrome. Arch Dis Child Fetal Neonatal Ed 102 (6), F497–F503.
Takahashi, H., Sano, H., Chiba, H., Kuroki, Y., 2006. Pulmonary surfactant proteins A and D: innate immune functions and biomarkers for lung diseases. Curr Pharm Des 12 (5), 589–598.
Tchoreloff, P., Gulik, A., Denizot, B., Proust, J.E., Puisieux, F., 1991. A structural study of interfacial phospholipid and lung surfactant layers by transmission electron microscopy after Blodgett sampling: influence of surface pressure and temperature. Chemistry and Physics of Lipids 59 (2), 151–165.
Thai, L.P., Mousseau, F., Oikonomou, E., Radiom, M., Berret, J.F., 2020. Effect of Nanoparticles on the Bulk Shear Viscosity of a Lung Surfactant Fluid. ACS Nano 14 (1), 466–475.
Thompson, K.C., Jones, S.H., Rennie, A.R., King, M.D., Ward, A.D., Hughes, B.R., Lucas, C.O., Campbell, R.A., Hughes, A.V., 2013. Degradation and rearrangement of a lung surfactant lipid at the air-water interface during exposure to the pollutant gas ozone. Langmuir 29 (14), 4594–4602.
Valle, R.P., Huang, C.L., Loo, J.S.C., Zuo, Y.Y., 2014. Increasing Hydrophobicity of Nanoparticles Intensifies Lung Surfactant Film Inhibition and Particle Retention. ACS Sustainable Chemistry & Engineering 2 (7), 1574–1580.
Valle, R.P., Wu, T., Zuo, Y.Y., 2015. Biophysical influence of airborne carbon nanomaterials on natural pulmonary surfactant. ACS Nano 9 (5), 5413–5421.
Veldhuizen, R., Nag, K., Orgeig, S., Possmayer, F., 1998. The role of lipids in pulmonary surfactant. Biochimica et Biophysica Acta (BBA) - Molecular Basis of Disease 108.

Waisman, D., Danino, D., Weintraub, Z., Schmidt, J., Talmon, Y., 2007. Nanostructure of the aqueous form of lung surfactant of different species visualized by cryo-transmission electron microscopy. Clin Physiol Funct Imaging 27 (6), 375–380.
Walther, F.J., Gordon, L.M., Waring, A.J., 2016. Design of Surfactant Protein B Peptide Mimics Based on the Saposin Fold for Synthetic Lung Surfactants. Biomed Hub 1 (3).
Walther, F.J., Gordon, L.M., Waring, A.J., 2019. Advances in synthetic lung surfactant protein technology. Expert Rev Respir Med 13 (6), 499–501.
Warriner, H.E., Ding, J., Waring, A.J., Zasadzinski, J.A., 2002. A Concentration-Dependent Mechanism by which Serum Albumin Inactivates Replacement Lung Surfactants. Biophysical Journal 82 (2), 835–842.
Weaver, T.E., Na, C.L., Stahlman, M., 2002. Biogenesis of lamellar bodies, lysosome-related organelles involved in storage and secretion of pulmonary surfactant. Semin Cell Dev Biol 13 (4), 263–270.
Weber, K., Razinger, T., Hardisty, J.F., Mann, P., Martel, K.C., Frische, E.A., Blumbach, K., Hillen, S., Song, S., Anzai, T., et al., 2011. Differences in rat models used in routine toxicity studies. Int J Toxicol 30 (2), 162–173.
Whitsett, J.A., Nogee, L.M., Weaver, T.E., Horowitz, A.D., 1995. Human surfactant protein B: structure, function, regulation, and genetic disease. Physiol Rev 75 (4), 749–757.
Willson, D.F., Notter, R.H., 2011. The future of exogenous surfactant therapy. Respir Care 56 (9), 1369–1386 discussion 1386–1368.
Wright, J.R., 1997. Immunomodulatory functions of surfactant. Physiol Rev 77 (4), 931–962.
Wu, M., Wang, F., Chen, J., Zhang, H., Zeng, H., Liu, J., 2022. Interactions of model airborne particulate matter with dipalmitoyl phosphatidylcholine and a clinical surfactant Calsurf. J Colloid Interface Sci 607 (Pt 2), 1993–2009.
Xu, L., Yang, Y., Simien, J.M., Kang, C., Li, G., Xu, X., Haglund, E., Sun, R., Zuo, Y.Y., 2022. Menthol in electronic cigarettes causes biophysical inhibition of pulmonary surfactant. Am J Physiol Lung Cell Mol Physiol 323 (2), L165–L177.
Yang, Y., Xu, L., Dekkers, S., Zhang, L.G., Cassee, F.R., Zuo, Y.Y., 2018. Aggregation State of Metal-Based Nanomaterials at the Pulmonary Surfactant Film Determines Biophysical Inhibition. Environ Sci Technol 52 (15), 8920–8929.
Young, S.L., Fram, E.K., Larson, E.W., 1992. Three-dimensional reconstruction of tubular myelin. Exp Lung Res 18 (4), 497–504.
Yue, K., Sun, X., Tang, J., Wei, Y., Zhang, X., 2019. A Simulation Study on the Interaction Between Pollutant Nanoparticles and the Pulmonary Surfactant Monolayer. Int J Mol Sci 20 (13).
Yue, T., Xu, Y., Li, S., Luo, Z., Zhang, X., Huang, F., 2017. Surface patterning of single-walled carbon nanotubes enhances their perturbation on a pulmonary surfactant monolayer: frustrated translocation and bilayer vesiculation. RSC Advances 7 (34), 20851–20864.
Yue, T., Xu, Y., Li, S., Luo, Z., Zhang, X., Huang, F., 2017. Ultrashort Single-Walled Carbon Nanotubes Insert into a Pulmonary Surfactant Monolayer via Self-Rotation: Poration and Mechanical Inhibition. J Phys Chem B 121 (13), 2797–2807.
Zhao, Q., Li, Y., Chai, X., Zhang, L., Xu, L., Huang, J., Ning, P., Tian, S., 2019a. Interaction of nano carbon particles and anthracene with pulmonary surfactant: The potential hazards of inhaled nanoparticles. Chemosphere 215, 746–752.
Zhao, Q., Wang, Q., Li, Y., Ning, P., Tian, S., 2019b. Influence of volatile organic compounds (VOCs) on pulmonary surfactant monolayers at air-water interface: Implication for the pulmonary health. Colloids and Surfaces A: Physicochemical and Engineering Aspects 562, 402–408.
Zhao, Q., Li, Y., Chai, X., Xu, L., Zhang, L., Ning, P., Huang, J., Tian, S., 2019c. Interaction of inhalable volatile organic compounds and pulmonary surfactant: Potential hazards of VOCs exposure to lung. J Hazard Mater 369, 512–520.
Zucco F, De Angelis I, Stammati A: **Cellular Models for In Vitro Toxicity Testing**. In: *Animal Cell Culture Techniques*. 1998: 395-422.
Zuo, Y.Y., Veldhuizen, R.A., Neumann, A.W., Petersen, N.O., Possmayer, F., 2008. Current perspectives in pulmonary surfactant–inhibition, enhancement and evaluation. Biochim Biophys Acta 1778 (10), 1947–1977.